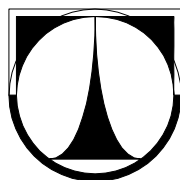

TECHNICAL UNIVERSITY OF LIBEREC

Faculty of Mechatronics and Interdisciplinary Engineering Studies



Course of study: M 2612 Electrical Engineering and Informatics

Field of study: 3906T001 Mechatronics

Testování mnohokanálových fotonásobičů pro detektor čerenkovského záření Compass - RICH

Tests of a multianode photomultipliers for the RICH detector

DIPLOMA THESIS

Author: Lukáš Steiger

Supervisor: Doc. Rndr. Miroslav Šulc, Ph.D.

Consultant: Ing. Miloš Slunečka

Liberec 19. 5. 2006

Prohlášení

Byl(a) jsem seznámen(a) s tím, že na mou diplomovou práci se plně vztahuje zákon č. 121/2000 o právu autorském, zejména § 60 (školní dílo).

Beru na vědomí, že TUL má právo na uzavření licenční smlouvy o užití mé diplomové práce a prohlašuji, že **s o u h l a s í m** s případným užitím mé diplomové práce (prodej, zapůjčení apod.).

Jsem si vědom(a) toho, že užití své diplomové práce či poskytnout licenci k jejímu využití mohu jen se souhlasem TUL, která má právo ode mne požadovat přiměřený příspěvek na úhradu nákladů, vynaložených univerzitou na vytvoření díla (až do jejich skutečné výše).

Diplomovou práci jsem vypracoval(a) samostatně s použitím uvedené literatury a na základě konzultací s vedoucím diplomové práce a konzultantem.

Datum

Podpis

Acknowledgements

I would like to express my gratitude to my university supervisor Miroslav Šulc for his support and professional leading.

Also I would like to express my gratitude to Miloslav Slunečka for his very useful advises regarding my thesis and for the help I received during the process of conducting the tests.

My thanks belong also to Miroslav Finger from Charles University in Prague and especially to Andreas Teufel from Friedrich-Alexander University in Erlangen-Nurnberg for his patience and technical assistance we received during the process of conducting the tests.

I would like to thank to all Czech group members for their enjoyable and RICH cooperation during the process of testing.

Abstrakt

Detektor RICH1 (Ring Imaging CHerenkov) je důležitou součástí experimentu Compass, který probíhá v Evropské Laboratoři pro částicovou fyziku (CERN). Centrální část detektoru fotonů, původně s fotokatodou z CsI, bude vyměněna za pole velmi rychlých vícekanálových fotonásobičů firmy Hamamatsu s rozšířenou citlivostí v UV oblasti.

Tato práce se zabývá testováním vícekanálových fotonásobičů, a v neposlední řadě také zpracováním výsledků testů.

Teoretická část se věnuje popisu fotonásobičů. Je zde obsaženo i stručné vysvětlení detektoru RICH1 a popis měřicí aparatury.

Praktická část se zabývá naměřenými výsledky a jejich zpracováním. Mezi vlastnosti fotonásobičů, které byly zkoumány, patří temnotní proudy, kvantová účinnost, tvar signálu a stejnorodost kanálů v rámci jednoho fotonásobiče. Veškerá měření probíhala ve fyzikálním ústavu, jenž je součástí Friedrich-Alexanderské University v Erlangenu.

Klíčová slova:

Detektor RICH

Fotonásobič

Abstract

The aim of this thesis is to check and classify multi-anode photomultipliers which will be used as a part of the read-out system of the RICH detector. The RICH detector is a part of the Compass experiment, which is being upgraded at the European Laboratory for Particle Physics (CERN) in Geneva.

The theoretical part contains a description of the photomultipliers and basic information about upgrading the RICH detector. Used control and measuring apparatus is also described.

The experimental part is aimed on the retrieved results and their processing. Testing of multi-anode photomultipliers and first data processing took place at the Friedrich-Alexander University of Erlangen-Nürnberg. The main tested parameters of the photomultipliers were dark current in each channel, relative quantum efficiency, signal shape and uniformity of the channels. All measurements (except dark current measurement) were made for two wavelengths and different voltages.

Keywords:

RICH detector

Photomultiplier

Contents

Introduction	9
1 Theoretical Part	10
1.1 The Compass experiment at CERN.....	10
1.2 RICH detector.....	11
1.2.1 RICH detector principle.....	11
1.2.2 RICH1 upgrade.....	12
1.3 General description of the PMT	14
1.3.1 Photomultiplier structure	14
1.3.2 Characteristics of Photomultiplier tubes	18
2 Practical Part.....	21
2.1 Multi-anode photomultiplier tube	21
2.2 Experimental apparatus	23
2.2.1 Measurement method	24
2.2.2 Light Source	30
2.2.3 Electronic Equipment	31
2.2.4 Results.....	32
3 Discussion.....	47
Conclusions	50
Literature	51

Introduction

COMPASS (COmmon Muon Proton Apparatus for Structure and Spectroscopy) setup is the largest fixed target particle physics experiment in CERN (European Organization for Nuclear Research). During the year 2005 and spring 2006, several of its subsystems undergo major upgrades targeted mainly to the response increase [1].

RICH1 (Ring Imaging Cherenkov Detector) is used for particle identification by measuring their velocity by means of emitted Cherenkov light transformed into circles, composed of just few photons each. Central part wire-chambers with CsI layers used in the past as photon detectors are going to be replaced by an array of much faster MAPMTs (Multi-Anode Photomultiplier Tubes).

Number of multi-anode photomultiplier tubes to be used in the RICH environment is 594. Therefore some properties of PM tubes have to be checked to confirm what manufacturer presents, to obtain individual characteristics of each of them and to be sure that PM tubes are ready to use. Our team ensures visual inspection, dark current measurement before and after illumination, relative quantum efficiency measurement. Also we studied signal shape, uniformity and gain of each tube. Operational parameters of tubes are chosen on the basis of these tests. I was responsible for evaluation of 150 PMTs. I helped with the preparation of measuring apparatus and testing of the first trial set of PMTs in August 2005. Finally I participate in processing and qualification of all measured PMTs data.

1 Theoretical Part

1.1 The Compass experiment at CERN

The COMPASS experiment is a high luminosity experiment dedicated to hadron physics, with a full research programme including studies about nucleon spin structure and charm spectroscopy. The Compass experiment unites over 200 specialists from all over the world, including Czech group which consists of Technical University of Liberec, Faculty of Mathematics and Physics (Charles University in Prague), Czech Technical University in Prague, Institute of Scientific Instruments Brno (Academy of Science of the Czech republic).

The Compass experiment take place in CERN using a high intensity SPS (Super Proton Synchrotron) beam of polarized muons (or hadrons) interacting with two fixed targets composed of ${}^6\text{LiD}$. The nucleons inside the target material are polarized to a certain level and the target is kept at cryogenic temperatures (5mK) inside a solenoid or dipole magnet. The aim of this experiment is to identify originated particles and to define their properties.



Figure 1.1 *Drawing of the Compass setup.*

The system uses two spectrometer magnets to deviate charged particles and several types of particle detection systems to enable high precision particle tracking in space and time, electromagnetic and hadronic calorimetry and muon detection. Energy is measured by Calorimeters (ECAL, HCAL – see Fig. 1.1), trajectory is measured by system of tracking detectors (Tracking – see Fig. 1.1). The RICH detector serves to identify particles and to find out their velocity and momentum.

1.2 RICH detector

1.2.1 RICH detector principle

For particle detection is used phenomenon called Cherenkov light. Particles moving through the dielectric media faster than the velocity of light in the medium emit a faint electromagnetic radiation at an angle related to the index of refraction of the media. If the charged particle moves at the conditions stated above, it can emit Cherenkov radiation with constant conical wavefront with angle depending only upon its velocity and the index of refraction of the medium [2].

Main part of the RICH detector is a gas-filled vessel with a structure of mirrors transforming the Cherenkov light cones into the spherical wavefronts focalized onto the system of photon detectors in the mirrors focal plane. These light cones create circles on the detectors. Diameter and centre of the circle gives us information about velocity and direction of the particle. Principled schema is shown on the Figure 1.2.

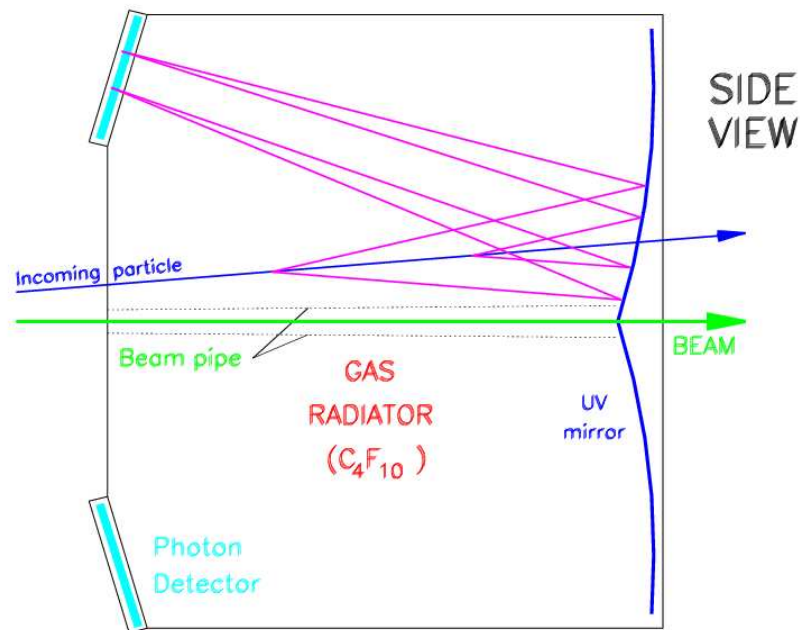


Figure 1.2 Principle of the RICH detector.

1.2.2 RICH1 upgrade

RICH1 detector is the largest and the most difficult detector used in the Compass experiment. The photon detection part is equipped with 8 Multi Wire Proportional Chambers (MWPC) [3] with large size CsI photocathodes allowing the single photon detection. The sensitive area covers 5.3 m² in total.

The RICH1 upgrade consists of two complementary objects. Firstly, it is necessary to reduce the detector dead time, so the read-out electronics upgrade is needed. The second object is to upgrade the central part of the RICH1 detector (Fig. 1.3). New system will be based on multi-anode photomultiplier tubes with focusing lenses. This system together with reduced dead time read-out system will result in an important increase in the number of detected photons and in a reduction of the background from uncorrelated events [1].

The MAPMTs (Multi-Anode Photomultiplier Tubes) chosen are the R7600-03-M16 by Hamamatsu. This PMT is characterized by a bialkali photocathode with 18 x 18 mm² active surface, 16 pads and UV extended glass entrance window to increase the range of the detectable Cherenkov light spectrum (200 – 600 nm) [3]. The area covered by one photomultiplier will be 48x48 mm² and 12x12 MAPMTs will be placed in each of four specially designed frames. It was produced 594 systems to have some spare elements.

MAPMTs are coupled to a two lens system that allows increasing the geometrical acceptance and to minimize image distortion. Lenses are made of fused silica in order to match the wavelength range of the PMT [2].

Experiment should start in the summer of 2006.

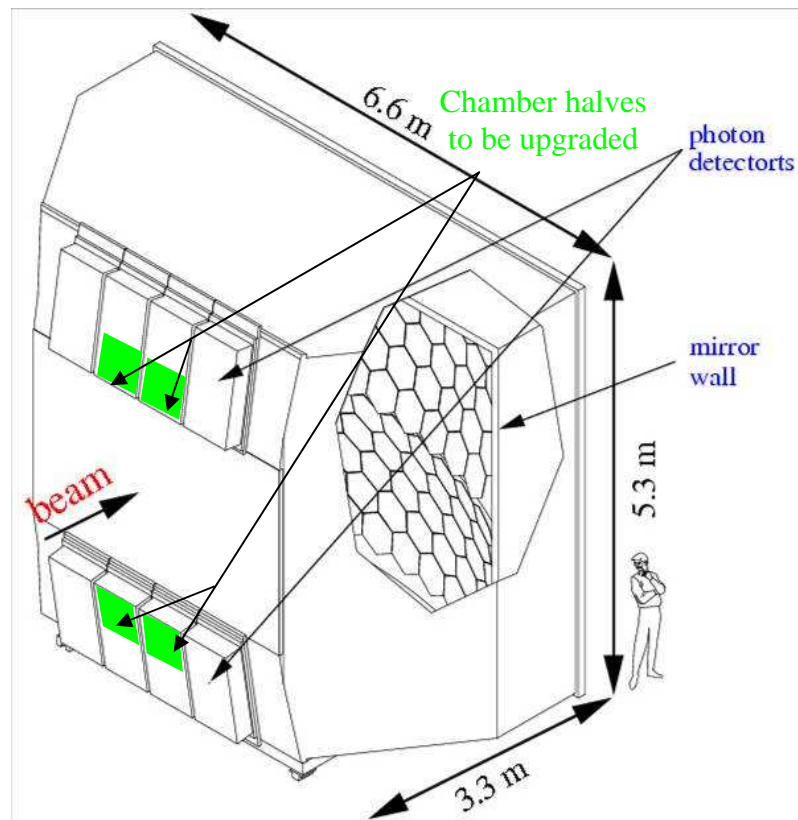


Figure 1.3 Rich detector.

1.3 General description of the PMT

1.3.1 Photomultiplier structure

Photomultipliers are special tools developed and used for a scintillation counting in radiation detection and spectroscopy where the weak light output occurs. So, PMT converts extremely weak light signal into a corresponding electrical signal. Usually, this light signal typically consists of no more than a few hundred photons [4].

We can find PMTs of various designs but generally, all consist of a photocathode, a photoelectron collection region between the photocathode and the first dynode, a multistage electron multiplier section, and an anode for collection of the amplified charge. These structures are enclosed in a glass vacuum envelope. (This simplified structure can be seen on Fig. 1.4)

Photomultiplier's major components are photocathode coupled to an electron multiplier structure.

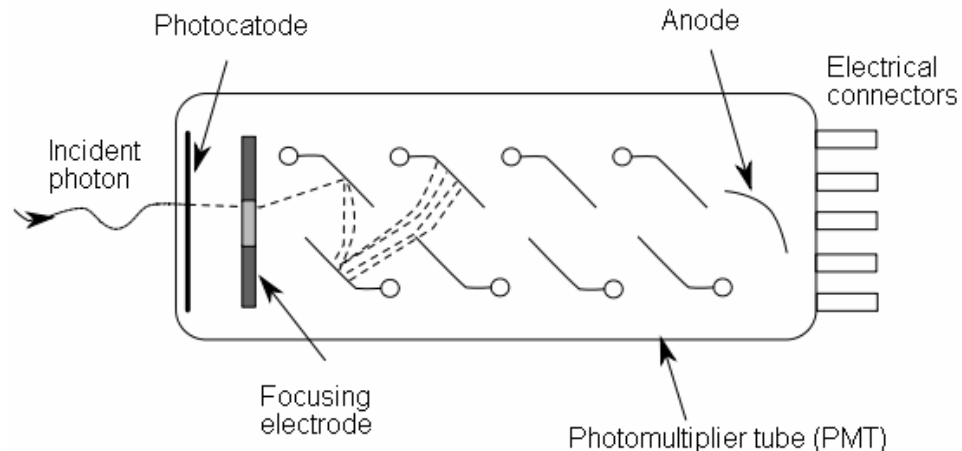


Figure 1.4 Basic elements of a PM tube.

Photocathode

Photocathode is a photosensitive layer which serves to convert as many of the incident light photons as possible into low-energy electrons. PM tubes are sensitive to radiant energy in the ultraviolet, visible and near-infrared regions of the electromagnetic

spectrum. This sensitivity is mainly influenced by the photocathode, because the conversion of incident light photon into electrons requires enough energy (Fig. 1.5). Incident photon has to be firstly absorbed. Then, within the photoemissive material, the energy is transferred to an electron. In next step, electron migrates to the surface where the escape of the electron from the surface should happen. Energy of the photon is given by *quantum energy of the photon* $E(eV)$ (Eq. 1-1).

$$E = h \cdot \nu = h \cdot \frac{c}{\lambda} \qquad \text{Eq. 1-1}$$

h ... Planck's constant ($6.26 \times 10^{-34} \text{Js}$)

ν ... Frequency of light (Hz)

c ... Velocity of light ($3 \times 10^8 \text{ms}^{-1}$)

But some energy is lost through electron-electron collision in the migration process. In third step, there must be sufficient energy to overcome potential barrier [5]. This potential barrier depends on the material from which the photosensitive layer is made and always exists at any interface between material and vacuum. Suitably prepared semiconductors are much better than most metals [4]. Also the rate of energy loss as the electron migrates is dependent on used material and the rate of energy loss for metals is relatively high in comparing with semiconductors. So called escape depth (it is a depth at which electrons may originate and still reach the surface with sufficient energy to overcome the potential barrier) can extend to about 25 nm in semiconductors. But photocathodes of this thickness are semitransparent and it will cause that less a half the visible light to interact within the photosensitive layer.

Wavelength	Spectral Range	Frequency	Energy
nm		(Hz)	(eV)
10	X-ray Soft X-ray		
10 ²	Extreme UV region	10 ¹⁶	10 ²
200		Vacuum UV region	
350	Ultraviolet region	10 ¹⁵	10
750	Visible region		
10 ³	Near infrared region		1
10 ⁴	Infrared region	10 ¹⁴	
10 ⁵			10 ¹³
10 ⁶	Far infrared region		10 ⁻²
			10 ¹²

Figure 1.5 Spectral regions and unit conversion. [7]

Photocathodes can be constructed as either opaque or semitransparent layers. PMTs that we used to work with are semitransparent. They are also more common in PM tubes designed for scintillation counters because they are more readily adaptable to tube designs that use flat end window. Thus, let limit oneself to a few word that each type is used in different geometric arrangement and we will discuss only the photocathode with semitransparent layer. They generally are no thicker than the escape depth and are deposited on a transparent backing. Light first passes through the transparent backing and subsequently into the photocathode layer, photoelectrons are collected from the opposite surface to which the light is incident.

Multistage electron multiplier section

Electron multiplier structure serves as a near-ideal amplifier to increase number of produced electrons to usable current [6]. The output charge from the photocathode is too low to serve as a convenient electrical signal because only few hundred electrons may be involved in a typical pulse. After amplification through the multiplier structure, a typical scintillation pulse will give rise to 10⁷-10¹⁰ electrons which is sufficient.

The multiplier function is based on the phenomenon of secondary electron emission [4]. Electrons leaving the photocathode are accelerated and caused to strike the surface of an electrode, called *dynode*. This phenomenon is very similar to the photoemission process. However, in this case, electrons within the dynode material are excited by the passage of the energetic electron originally incident on the surface rather than by an optical photon. Electrons leaving the photocathode are attracted to the first dynode and produce a definite number of electrons for each incident photoelectrons. Electrons that are produced at the surface of the first dynode have very low energies, typically a few eV . Then low-energy secondary electrons from dynode are accelerated toward the following dynode thanks to electrostatic field established between the dynode and following similar dynode. This process can be repeated many times. Thus, overall gain depends on the number of stages (dynodes) that are used. Also the overall gain of a PMT is a sensitive function of applied voltage [7].

An external voltage source must be connected to the PM tubes in such a way that the photocathode and each following multiplier stage are correctly biased with respect to one another. Because electrons must be attracted, the first dynode must be held at a positive voltage with respect to the photocathode, and each following dynode must be held at a positive voltage with respect to preceding dynode.

Shielding

Photomultiplier tube characteristics may vary with external electromagnetic fields, ambient temperature, humidity, or mechanical stress to the tube. For this reason it is necessary to use a magnetic or electric shield that protects the tube from such adverse environmental factors (Even the influence of the earth's magnetic field is sufficient to have an appreciable effect on the trajectories of electrons inside the tube). Next function of the housing is to shield extraneous light (for instance, when the connector is used for signal output/input, there is a possibility of light leakage through the connector itself etc.).

For most tube designs, this shield must be held at photocathode potential in order to avoid noise due to electroluminescence in the glass envelope. Moreover, a cooled housing is sometimes used to maintain the tube at a constant temperature [7].

1.3.2 Characteristics of Photomultiplier tubes

There are many ways to describe photomultiplier tubes (Fig. 1.6) properties. In this chapter only some characteristics or specifications will be described. (Only these, of our interest - like everywhere in this thesis).



Figure 1.6 Various types of photomultiplier tubes[8].

Quantum Efficiency (QE)

The photocathode of the photomultiplier tube is characterized by the quantum efficiency [4,10]. The quantum efficiency is defined as the ratio of the number of emitted photoelectrons to the number of incident photons (Eq. 1-2).

$$QE = \frac{N_{electrons}}{N_{photons}} \quad \text{Eq. 1-2}$$

The quantum efficiency would be 100% for an ideal photocathode. But practical photocathodes show maximum quantum efficiencies of 20-30%.

The quantum efficiency of any photocathode is also very strong function of wavelength or quantum energy of the incident light.

Dark Current

Dark current is an output current which is produced and measured even when operated in a completely dark state, thus, without photocathode illumination [4]. Of course this output current should be kept as small as possible. Dark current could be caused by Thermionic emission current from the photocathode and dynodes, leakage current between the anode and other electrodes inside the tube, photocurrent produced by scintillation from glass envelope or electrode support, field emission current, ionization current from residual gases (ion feedback), noise current caused by cosmic rays, radiation from radioisotopes contained in the glass envelopes and environmental gamma rays.

Dark current increases with an increasing supply voltage. Thermionic noise can be reduced by cooling the tube. But, when a photocathode is exposed to room illumination, the dark current strongly rises. The dark current will return to the original level by storing the tube in a dark state for one - two hours. However, if exposed to extremely intensive light, the tube may be damaged.

Gain

Current amplification is a question of the multiplier structure of the PMT and it is a function of the interstage voltage of dynodes. The electron multiplication factor remains constant for pulses over a wide range of incident light levels including the photon counting region. Nonlinearities can arise for very large pulses caused by space charge effects between the last dynode and anode where the number of electrons is greatest. Any deviation of dynode from their equilibrium value during the course of the pulse will also cause nonlinearity.

Uniformity

An important property of photocathodes is the uniformity to which their thickness can be held over the entire area of the photocathode. Variations in thickness give rise to corresponding changes in the sensitivity of the photocathode and can be one source of resolution loss in scintillation counters. The electron multiplier can be characterized by the uniformity as well.

We test multi-anode photomultipliers. So, in our case, the uniformity means the quantum efficiency difference between each channel of the PMT.

Pulse Timing properties

As it was already written, most photomultipliers perform charge amplification in a very linear manner, producing an output pulse at the anode that remains proportional to the number of original photoelectrons over a wide range of amplitude. Much of the timing information of the original light pulse is also retained. *The electron transit time* of a PM tube is defined as the average time difference between the arrival of a photon at the photocathode and the collection of the subsequent electron burst at the anode. Typical tube, when illuminated by a very short duration light pulse, will produce an electron pulse with a time width of a few nanoseconds after a delay time of 20-50ns [4]. More important quantity is *the spread in transit time*. It determines the time width of the pulse of electrons arriving at the anode of the tube. The amount of transit time spread observed for a specific pulse also depends on the number of initial photoelectrons per pulse.

The region between the photocathode and first dynode has influence on the timing properties of the PMT. There is a difference in paths between a photoelectron leaving the center of the photocathode and one at the edge. A second source of transit time spread arises from the distribution in initial velocities of photoelectrons leaving the photocathode.

2 Practical Part

2.1 Multi-anode photomultiplier tube

The project RICH1-upgrade is to improve the performance of the detector. Important factor is also the prize of this upgrade. Optical concentrators developed by Daniel Kramer [2] together with multi-anode photomultiplier tubes allow increasing the resolution of the detector. From this point of view, the use of conventional (non multi-anode) photomultiplier tubes is uneconomical in terms of both cost and space.

MA-PMTs couldn't be used in the past because the previous generation of such tubes suffered mainly from high crosstalk between channels and large channel-to-channel variations in gain. These drawbacks have been overcome with the H6568 model (Fig 2.1), multi-anode PMT developed by Hamamatsu Photonics [8]. Firstly H6568 was tested for usage in the HERA-B RICH detector [9]. This model, where the output signal is read out from independent multiple anodes, has greatly reduced drawbacks and combines such improvement with a very compact design.

The H6568 multi-anode PMT characterized by a bialkali photocathode with $18 \times 18 \text{ mm}^2$ active surface followed by 16 metal channel dynodes, each with 12 stages of mesh type and a multi-anode read-out. They are arranged as a 4×4 block. The compact design (overall dimension: $45 \text{ mm} \times 30 \text{ mm} \times 30 \text{ mm}$) is shown on the (Fig. 2.2). UV extended glass entrance window is used to increase the range (Fig. 2.3) of the detectable Cherenkov light spectrum (200 – 600 nm) [1]. Optical system, projected by Daniel Kramer in his thesis, carries out demands for deep ultra-violet range [2].

As it was already said, PMTs placed in the RICH1 detector will be coupled to a two lens system that allows increasing the geometrical acceptance and to minimize image distortions. Lenses are made from fused silica in order to match the wavelength range of the PMT. Time resolution of PMT is better than 130 ps. This resolution is ensured thanks to home made resistive dividers combined with other read-out electronics [1].



Figure 2.1 R5900-00-16 assembly (H6568)[7].

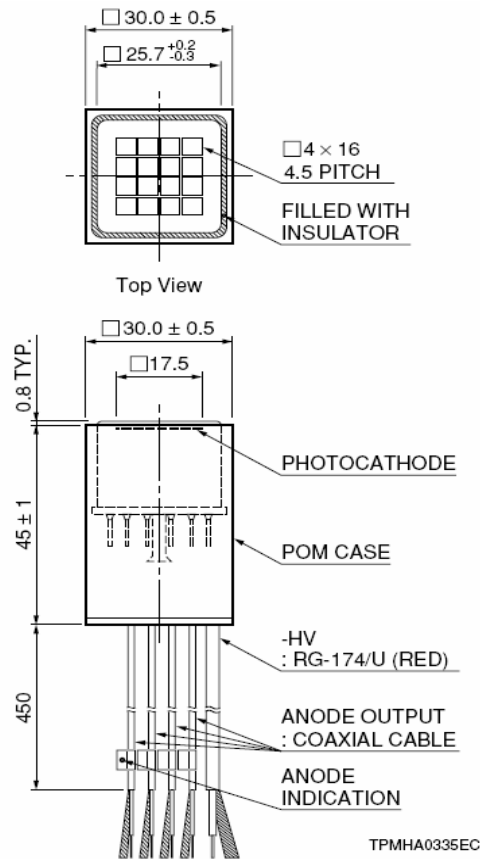


Figure 2.2 Layout and dimensions of the multi-channel photomultiplier tube H6568. The upper part shows the front view of the cathode grid [11].

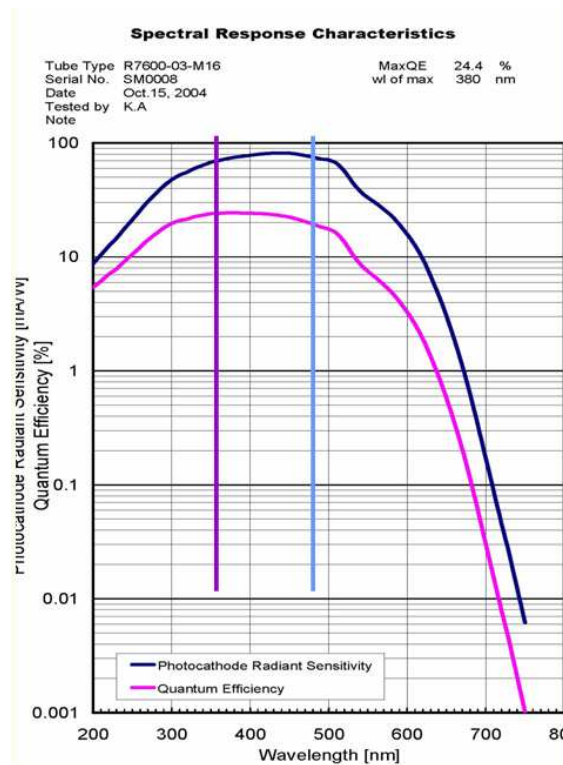


Figure 2.3 Spectral response of H6568. Two horizontal lines distinguish wavelength for diodes used in our tests[11].

Photomultipliers are stored in special housing from ferromagnetic material to prevent outer magnetic field. RICH1 detector is located in the residual field of one of the COMPASS magnets. The maximum value of magnetic field B in the region where the PMTs will sit is about 200 Gauss (and 1 Tesla = 10 000 Gauss). Inside the covering container, magnetic field is below 10 Gauss even for an external field around 200 Gauss [4]. And while B values are below 20 Gauss, there is no efficiency reduction.

2.2 Experimental apparatus

The aim of this diploma thesis is to measure overall quantum efficiency of the PMT for two different wavelengths and detected signal distribution for each channel. Next point is to measure dark current, gain of the PMT in a single-electron emission regime. All measurements are done for 596 multi-anode photomultipliers. This huge number requires good work and manpower organization. Data collection and all measurements were running in the laboratory of Friedrich-Alexander University in Erlangen-Nurnberg. All photomultiplier tests can be divided into two sections – data collection and data analysis.

For COMPASS users all files with measured data are accessible via the internet. In the first moment source files are shared. But in the future, all data will be accessible via the SQL database.

2.2.1 Measurement method

The measuring process could be divided into several steps (Fig. 2.4).

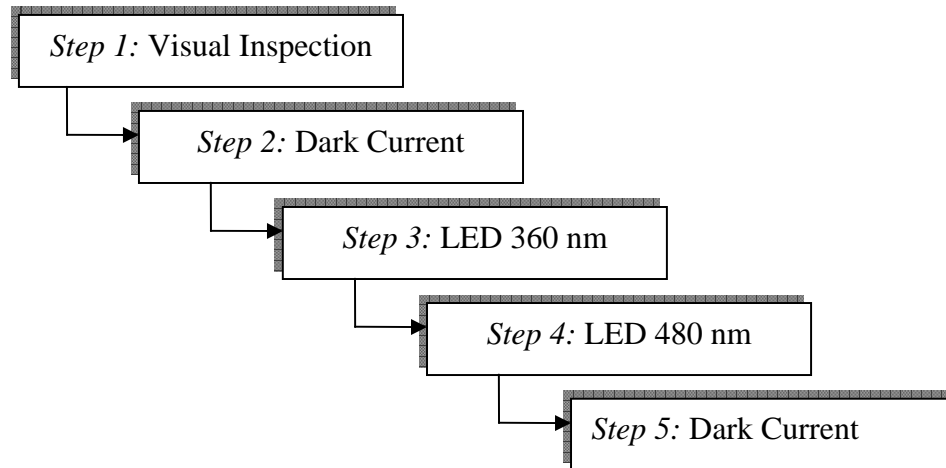


Figure 2.4 Steps of measurement

Photomultipliers were stored in small boxes. The first step starts with common visual inspection of the PMT (Fig. 2.5). We should check the power supply cable if it was broken and the PMT's envelope should be clean and unscuffed. If everything is OK, we could put the PMT into the black box (BB) (Fig. 2.6). The black box was especially prepared and constructed for this type of measurements. Whole box is black and light-tight inside. The only light that should occur is from light emitting diode. Special adjustments were made to obtain one photoelectron regime. We close the door and the measurement can begin.

Whole process of measurement is mostly automatic. One central computer is used to control whole process of measurements. Firstly Dark Current and Noise Rate are measured.

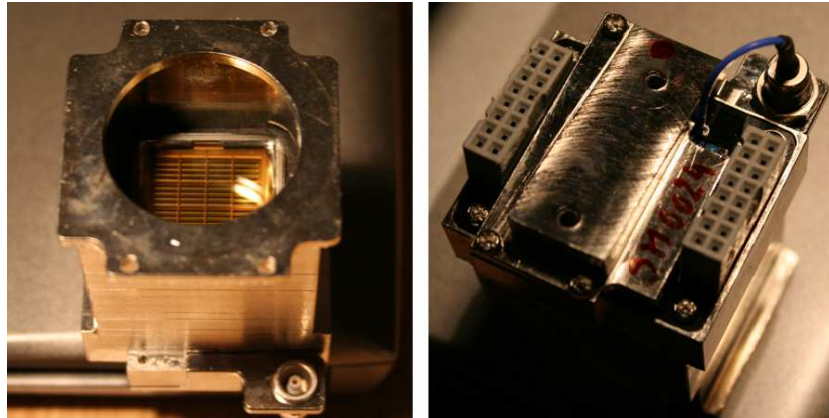


Figure 2.5 *Photomultiplier placed within its housing.*

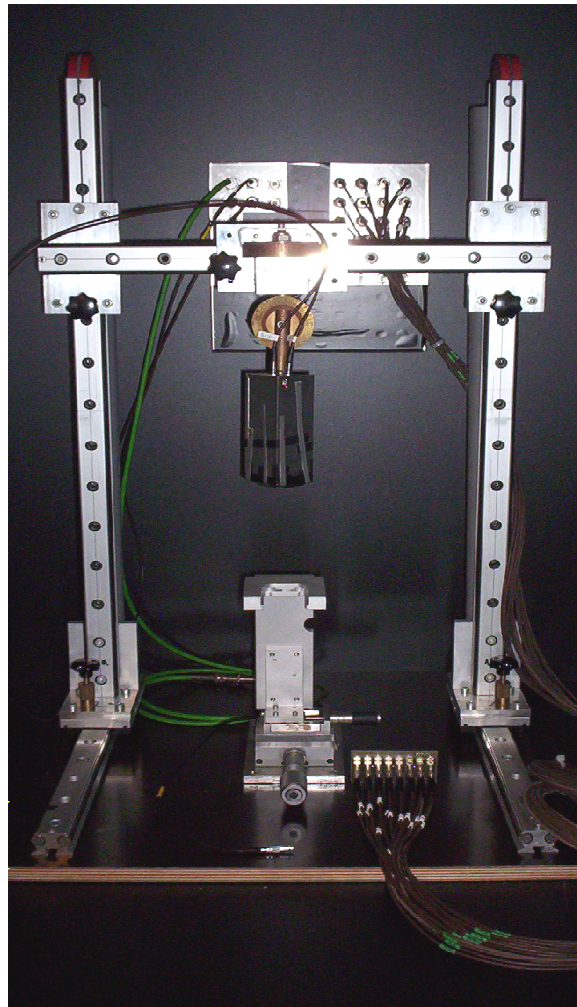


Figure 2.6 *Black Box with holder for PMT and Box for the LED.*

The PMT is very sensitive and so the PMT could gather some portion of charge during the time of PMT installation into a holder placed in BB. This charge could have some influence on upcoming measurements. To minimize its influence, the PMT was closed in BB for five minutes without any light.

When PMT is exposed to sunlight or extremely intense light (10 000 lux or higher), the tube may be damaged to some extent and not recoverable [7]. This should therefore be avoided. However, Hamamatsu assures that when a photocathode is exposed to room illumination, the Dark Current will return to its original level by storing the tube in a dark state for one - two hours. By considering the number of PMTs to be tested, two hours are not acceptable. So we tried to minimize photocathode illumination as well as possible (i.e. turn the light down, pull of a window blind and so on). During preliminary measurements we found that five minutes of dark state (for each PMT) are sufficient to reach low level of Dark Current. But it is valid only if light conditions described in previous sentence are kept (to extinguish illumination influence on photocathode).

After this period, the Dark Current was separately measured for each channel. The Keithley picoammeter (model no. 6485 – 5 ½ digit with 10fA resolution) was used for this type of measurements. Because Dark Current increases with an increasing supply voltage of the PMT (as shown on Fig. 2.7) the impress voltage was set to 970 V.

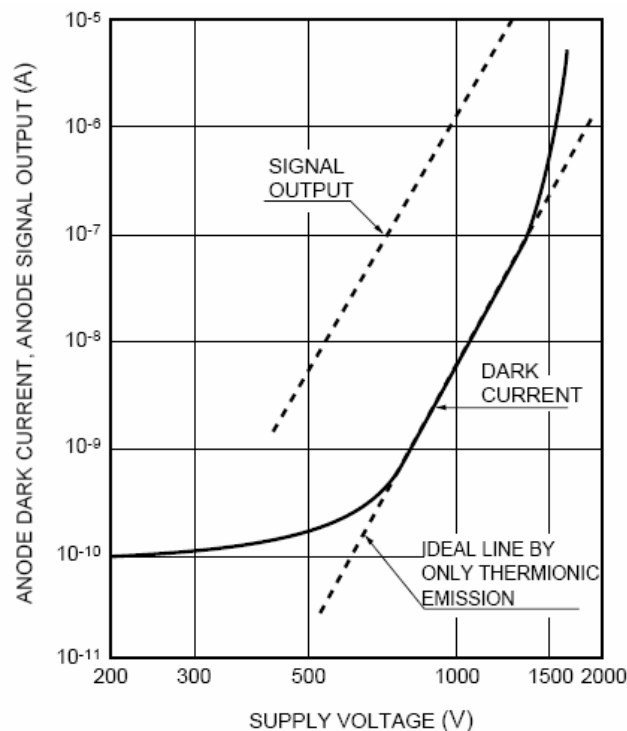


Figure 2.7 Typical Dark Current vs. supply voltage characteristic.

Dark Current measurement was under way twice, the first on the very beginning of whole measurement of one PMT and the second at the very end of the measurement again.

In the next step of the measurement signal shape, obtained uniformity and gain are checked for each channel of the PMT. LED diode (chapter 2.2.2) serves like our light source and is used in a pulse regime of 1 MHz.

The RICH detector set-up should allow detect the incident light which amount is minimal. Only few photons are expected. Tests of PMTs should be done in similar light conditions. Output light signal from the diode consists originally of huge number of photons. That's the purpose to make a special "housing" for used diodes (Fig. 2.8). This housing itself strongly reduces outgoing light from the LED. Also polarization filters are used to reduce light even more in the BB. Four polarization filters are fixed on the diode's housing. The aim was to get single photon regime.

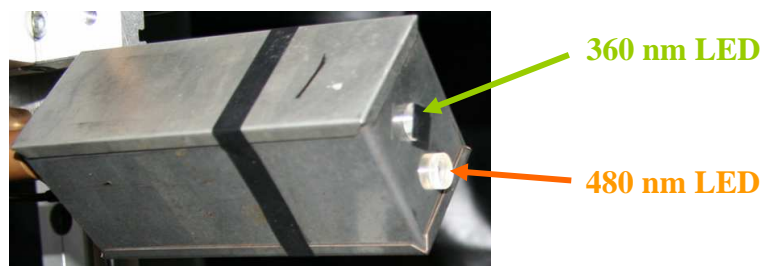


Figure 2.8 *Special housing for LED diodes to ensure minimal light output*

PMT's output impulse magnitude is proportional to energy of detected light as well as to applied voltage. It will be discussed later in this thesis (chapter 2.2.4). This step of measurement consists of five stages. 300 000 detected events are gathered in each stage. And each stage is measured for a different supply voltage (for 850/880/910/940/970 V).

The same type of measurement is done again, but with different LED diode. Used wavelengths are 360 nm and 480 nm (Fig. 2.8). LED diode with 480 nm wavelength serves like our light source in next step of the experiment. As was already said in the text before, PMTs are specially adapted to detect wavelengths between 200 nm and 600 nm. Only these types of diodes (360 nm and 480 nm) were accessible in given range. Of course we would like to know typical spectral response (the Quantum Efficiency behaviour due to whole range of expected wavelengths) of such PMT. And for this purpose a monochromator

would be an ideal solution. But the time for testing was strongly limited and furthermore diodes are very cheap source of light. Time is the main reason for using LED diodes. Typical spectral response of PMT is shown on figure 2.3. So we can measure two points from whole characteristic. Because we do not have number of emitted photons from the LED, we could compare only PMTs between themselves and PMT itself. This difference is called Relative Quantum Efficiency.

After this type of measurement the Dark Current is measured again under same conditions like it was described in step one.

Control procedure of measurement is done between the first and the second step of described data acquisition. Shape of signal of the PMT is measured and recorded. Digital camera is used to record images of the oscilloscope. Digital camera Canon EOS 350D is connected with computer via USB cable. To store images on the harddisk serves Canon utility called Zoom Browser Ex. Images are taken for each channel of the photomultiplier. We can handle this, because a special distributive board was made and used. Thus we were able to switch between automatic and hand-operated regime. During the manual regime, analog signal was sent into the scope. As we switched channels, change appeared on the scope and we could make a photo. During the auto regime, channels were switched automatically. It was controlled by personal computer.

The laboratory was equipped with four personal computers for data acquisition, data processing, one PC was used as main control system and one for taking images. Three of them were equipped with Linux operating system and the last one with WindowsXP.

Anode output signals of the MA-PMT were digitized with standard Camac modules (principled schema is shown on Fig. 2.9). NIM (Nuclear Instrument Module) crate ensured the modules feeding (chapter 2.2.3). Detected light was converted into an electrical impulse within PMT. This impulse was conducted through capacitor into an amplifier and analog-digital converter (ADC). In ADC, analog magnitude of signal amplitude was transformed into digital bit information. And these informations were read by computer through an interface and wrote on harddisk for further analysis.

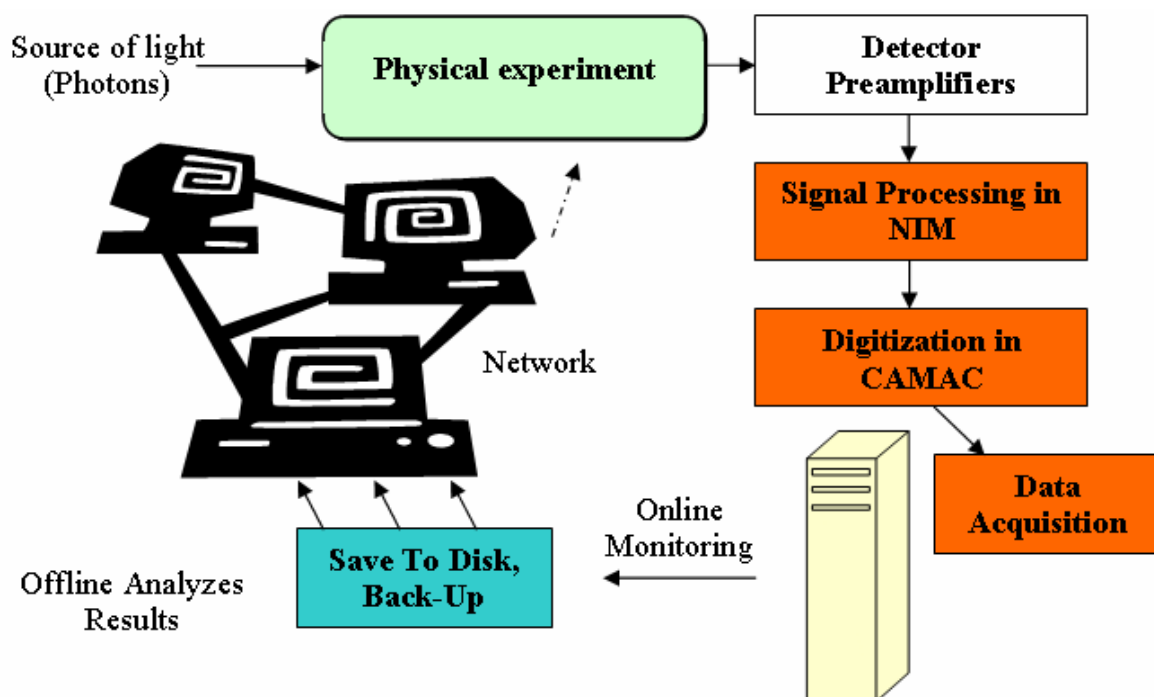


Figure 2.9 *Principled schema of data acquisition system.*

2.2.2 Light Source

Two Light Emitting Diodes (LEDs) are used for the generation of the pulsed light. During preliminary measurements we decided to use diodes with wavelengths 360 nm and 480 nm. Luminous spectra of LEDs are shown on Figure 2.10. 360 nm LED is the closest one to ultraviolet region from LEDs which were possible to get on the market.

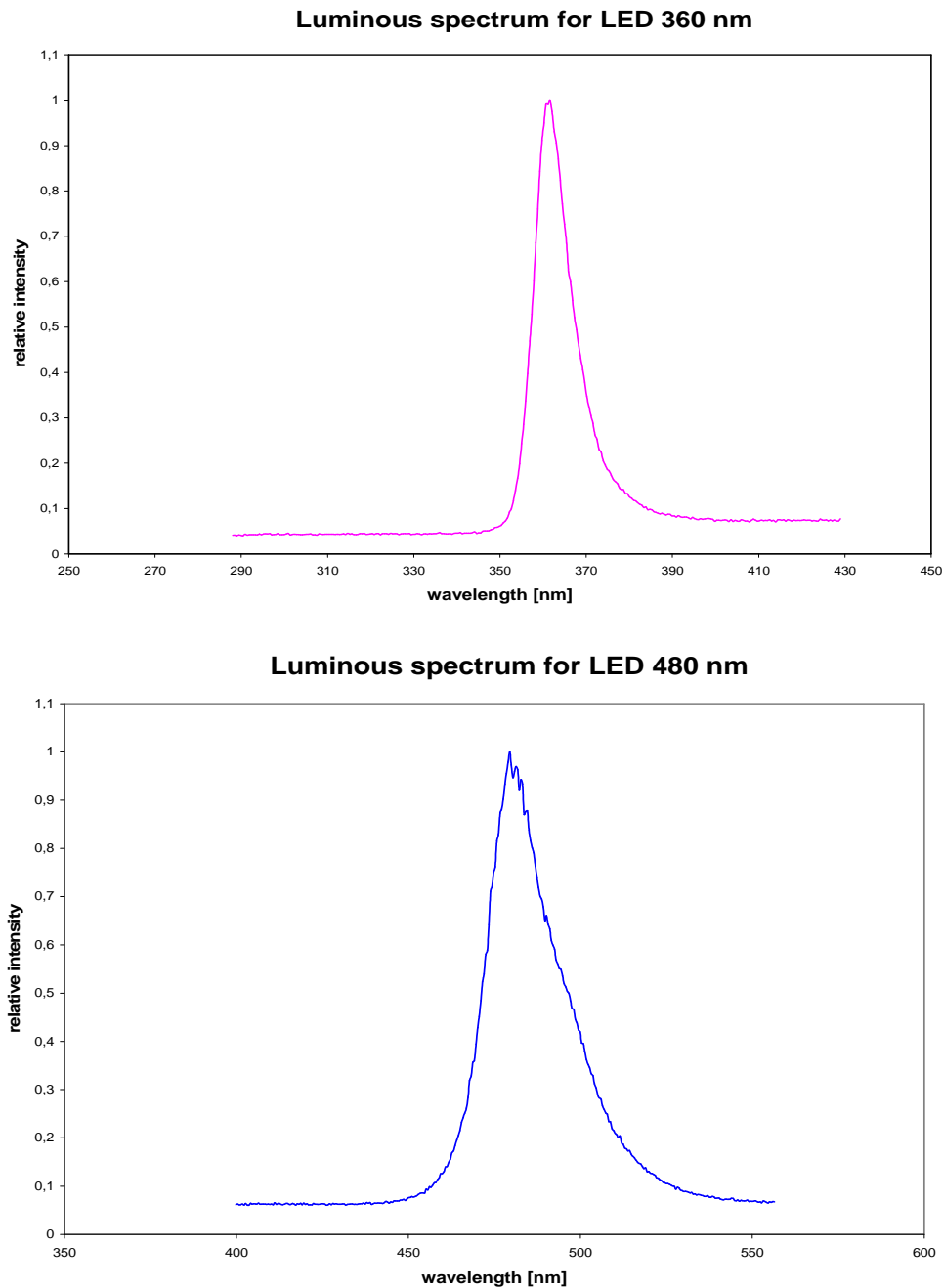


Figure 2.10 *Luminous spectra of LEDs – 360 nm & 480 nm*

2.2.3 Electronic Equipment

These equipments are used for data acquisition:

CAEN C 111A CAMAC Crate Controller – 16 bit interface for computer link used in single or multi CAMAC systems, up to 15 crates equipped with the C111A can be fully controlled from one interface, TTL logic, up to 500 kHz. It is interfaced with PC by a special card - *CAEN A151A TURBO*.

CAMAC Model 2249A – 12-Channel A-to-D Converter, resolution of ten bits to provide 0.1% resolution over a wide 1024-channel dynamic range, the input sensitivity of the is 0.25 pC/count for a full- scale range of 256 pC. Digitizing time is 60 μ s.

NIM Model 612A – 12-Channel Photomultiplier Amplifier with gain of ten. Rise time is less than 2 ns and delay is approximately 4 ns.

NIM BNC Model BL-2 – pulse generator

NIM N145 – Quad Scaler and Preset Counter – Timer

NIM Power supply Wenzel Elektronik N.1130-4 – programmable voltage supply for the photomultiplier, this module was connected with computer via parallel port.

Keithley picoammeter (model no. 6485) – 5 ½ digit with 10fA resolution, this picoammeter was also controlled with computer via RS232 interface.

Some photos are shown in the (appendix A).

2.2.4 Results

In this thesis is no place to show results of all 596 tested PMTs so there are shown only typical photomultipliers – representatives with high, normal and low or noisy signal (it depends on theme of each chapter). Outcome for each other PMT is accessible via internet for all compass users.

The yield of the PMT varies with the amount of incident light on photocathode. I mean the more photons will reach photocathode in one moment the more anode current will be. In our case, we had tried to reduce incident light until we reached the single photon regime. Firstly, this regime is closest to real conditions in the RICH detector. In this regime is also possible to find and set level for noise suppression. And if we reach single photon regime, it is possible to count the gain of PMT. Four polarization filters were experimentally turned and set to reduce light of the LED. After that we could take same light conditions for each PMT and for each step of measurement. Results were taken for all sixteen channels of one photomultiplier.

Dark Current

Dark Current is defined as anode current measured without photocathode illumination. Measurement of Dark Current was measured twice for each PMT. Dark Current was measured by Keithley picoammeter and automatically stored on harddisk. Typical picture of Dark Current outcome is shown for SM00144 PMT (Fig. 2.11).

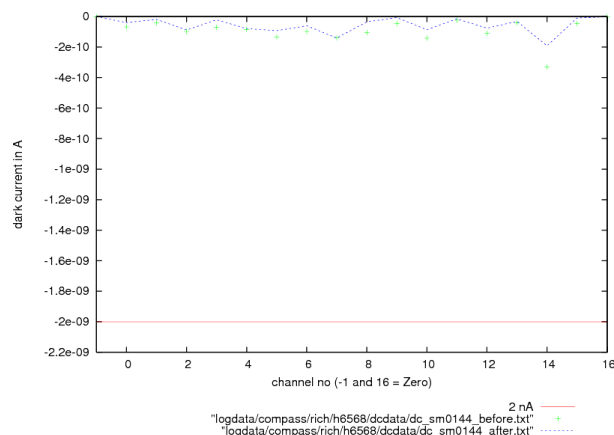


Figure 2.11 Dark Current of SM0144 before measurements (green cross) and after (dot line). Red line corresponds to maximum accepted value of Dark Current of PMT.

Spectral response

Spectral response is measured for five voltage values (for 850/880/910/940/970 V) and for two types of LEDs (360/480 nm). Typical spectral response is shown on figure 2.12. It is spectral response of PMT number SM0144 second channel for 970 V. This response corresponds to ideal PMT (at least ideal for as).

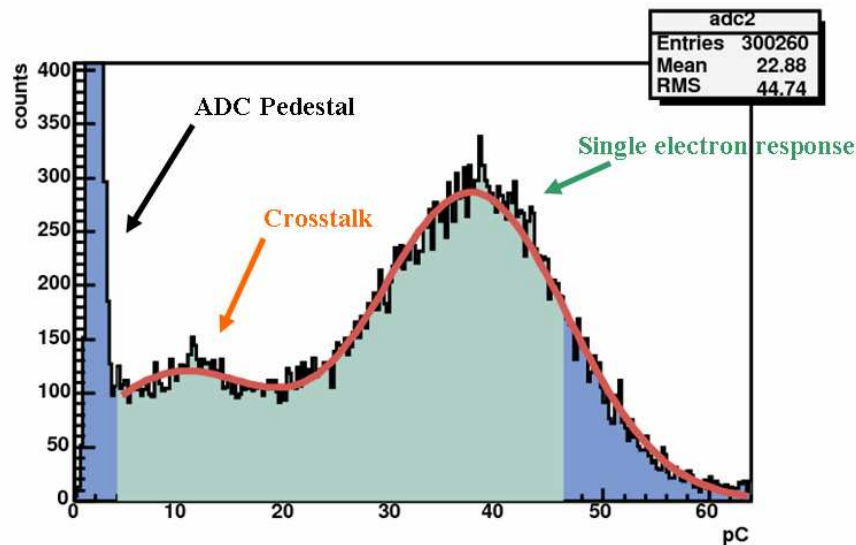


Figure 2.12 Spectral response of SM0144 PMT (2nd channel, 970 V).

On the histogram is shown anode charge versus number of events registered by analog-digital converter (ADC). Anode charge on the x-axis should be divided by ten to get real charge. It is caused by used amplifier (2.2.3).

Observed histogram could be divided into three parts. First part is called ADC Pedestal and is caused by adjusted zero within the ADC (for each channel). All values under this threshold will not be counted to PMTs events. Noise has mainly influence on the second part of the histogram. We assume that this part is mainly caused by crosstalks, thermionic emission and by Compton scattering (it is case when photon hands only proportion of his energy and then photon escapes or invokes additional interaction within photocathode. Third part, in other words main peak, corresponds to totally absorbed photons. One main peak is shown as single electron response. If there are more incident photons, on the picture will appear additional peaks behind this one (Fig 2.13). It depends on the number of absorbed photons.

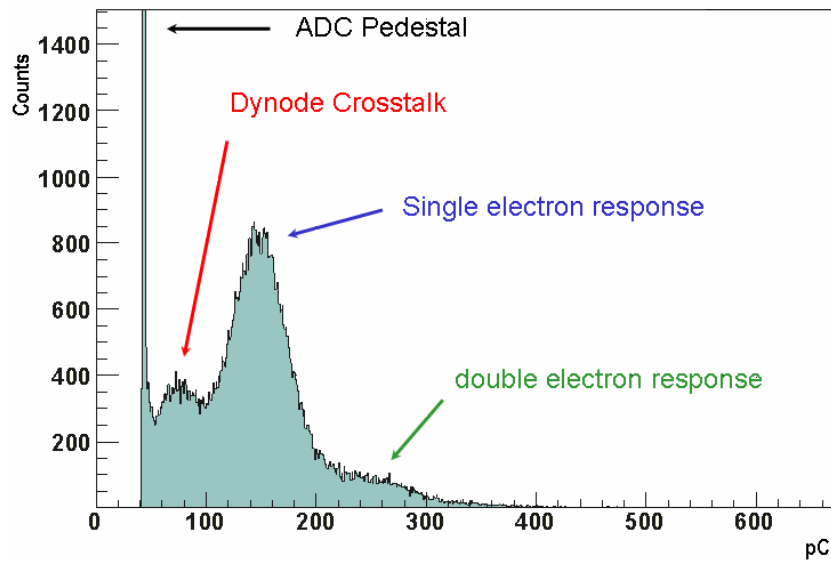


Figure 2.13 Spectral response with double electron response.

Finding an optimal setting including the light yield and number of events were also done during preliminary tests.

Raw data from the ADC are stored in files `<PMTs-name_wavelength_voltage.dat>`. Structure of the file is the same for each PMT. One row is one event so sum of rows corresponds to overall number of events. Columns correspond to individual channels. Therefore showed pictures are already analyzed data. The Root is used for it. It is an objected-oriented data analyzes framework based on C++ interpreter. Root allows interactive working (declarations or instructions of C++ language written from command line), running programs or macro (written in C++) and also in graphic regime Root allows to work interactively with created graphs. Root contains graphic editor and automatic generation of HTML documentation. Root is designed for effective large data processing (Root is developed in laboratories at CERN). The Root is also used to store mentioned file with smaller size as a `<PMTs-name_wavelength_voltage.root>`. Script for analyzing is attached on CD.

If the shape of examined PMT wasn't similar to shape that is shown on figure 2.12, it could mean some problems either with PMT itself or with the electronics. On figure 2.14 is shown channel one of SM309 PMT for 970 V with noisy signal. It is seen that the main peak and part of the histogram called crosstalks are not as well as differentiated as on figure 2.12.

As it could be assumed position of the main peak depends on anode charge magnitude. For higher outcome, the spectrum will be shifted to the right and for low signal

to the left. I mean that position of the mean value for main peak will change according to the gain of the PMT.

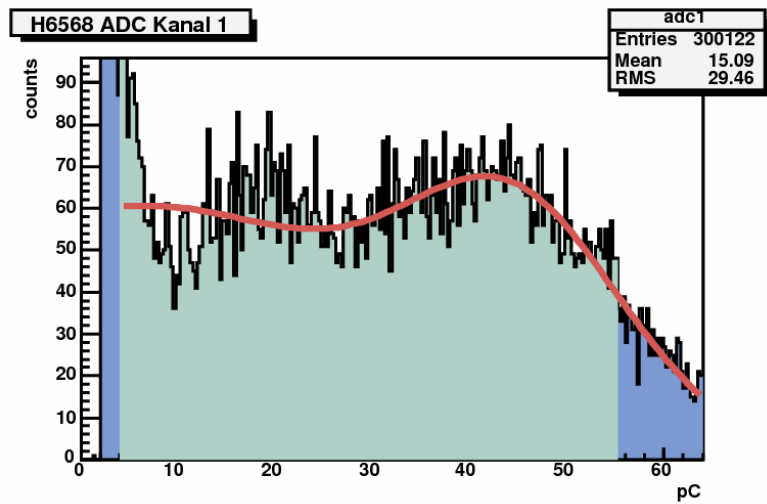


Figure 2.14 Spectral response with noisy signal.

Next figure (2.15) only present one of analysis outcome.

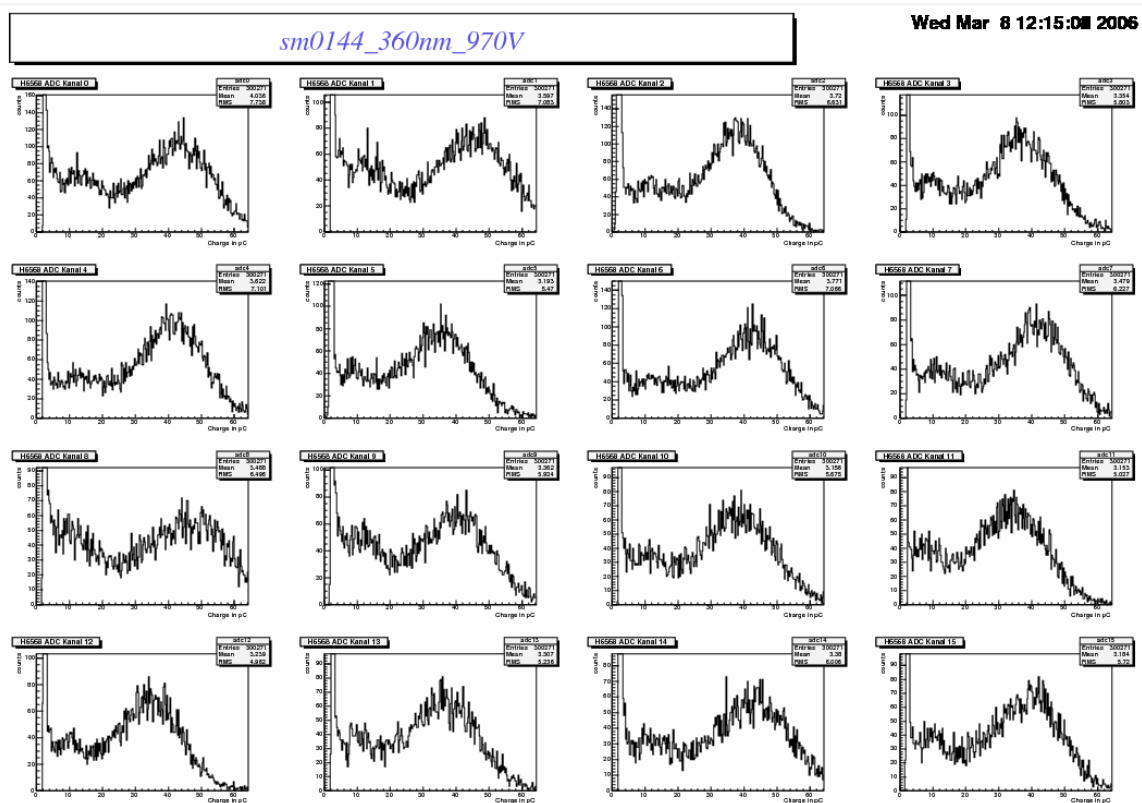


Figure 2.15 Spectral response of SM0144 photomultiplier for sixteen channels. These plots are stored like `<PMTs-name_wavelength_voltage.ps>`.

Also shape of PMT signal for each channel was recorded and stored on the harddisk (Fig 2.16).

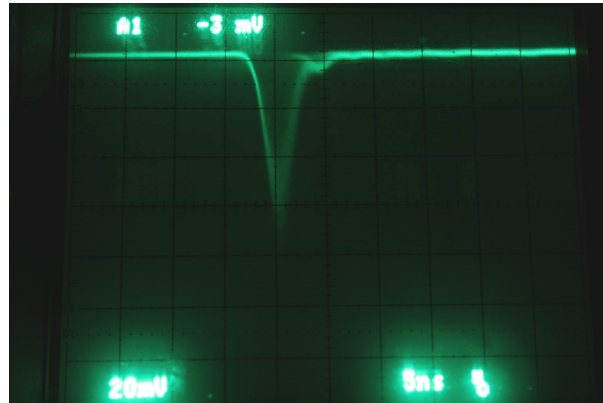


Figure 2.16 Shape of SM0144 channel 5.

These outcomes were very useful because bad channels or bad connectors were detected on the beginning of whole measurement. Images were taken of the scope. Also charge of signal could be counted from the shape. Charge of signal corresponds to area under the signal.

Gain of the PMT

Typical gain of H6568 photomultiplier is shown on figure 2.17.

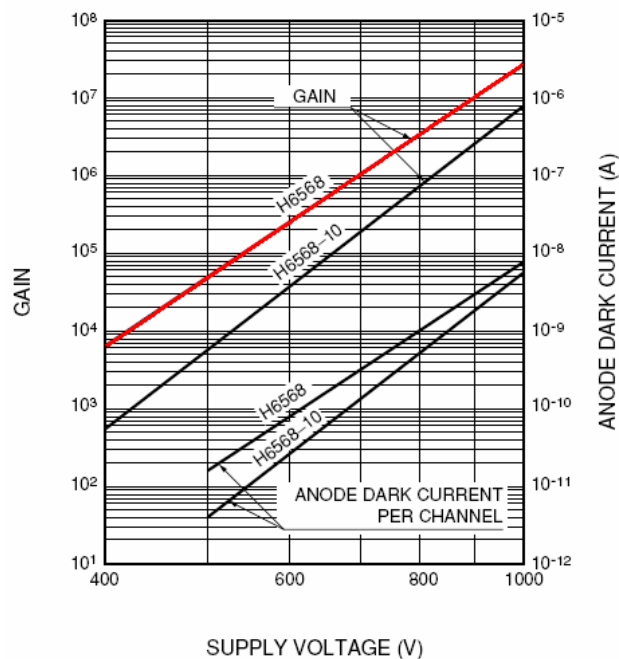


Figure 2.17 Typical Gain and Anode Dark Current of H6568 [11].

As we know, photoelectron current emitted from photocathode strikes the first dynode plane where secondary electrons are released. Then, each of these secondary electrons are accelerated up to upcoming dynode and multiplied again. So, primary photoelectron is multiplied in a cascade process from the first dynode up to the last one.

Our measurement was very specific in this step of measurement. Gain is defined as the ratio between photocathode and dynodes in general. But we were able to measure only anode output of PMT because its shielding. But as I mentioned earlier in this thesis we were working in single electron regime. And when we have the anode output I , the gain could be calculated in this way:

$$Gain = \frac{I_{out}}{I_{in}} \quad \text{Eq. 2-1}$$

I_{in} corresponds to one electron.

I_{out} is the value from the anode.

All outcomes except dark current measurement are expressed as anode charge in pC. That's the reason why I have decided to present the Y-axis in quantity of charge. The conversion is very simple:

$$1e^- = 1.602 \cdot 10^{-19} C \quad \text{Eq. 2-2}$$

Then

$$Gain = \frac{Q(U)}{Q(e^-)} \quad \text{Eq. 2-3}$$

$Q(U)$ is quantity of charge for specific voltage.

$Q(e^-)$ is quantity of charge for electron.

As we can see on figure 2.17 typical gain of H6568 is function of impress voltage. Typical values for our used voltage and gain converted into anode charge are written in the Table 2.1 :

High Voltage [V]	Gain [*10 ⁶]	Charge [pC]
850	6	1,0
880	8	1,3
910	10	1,6
940	16	2,6
970	20	3,2

Tab. 2.1 Gain dependence vs. Impress voltage.

Oncoming diagrams are shown for normal (Fig. 2.18 and Fig. 2.19), high (Fig. 2.20 and Fig. 2.21) and low (Fig. 2.22 and Fig. 2.23) signals for both types of diodes (360 nm and 480 nm).

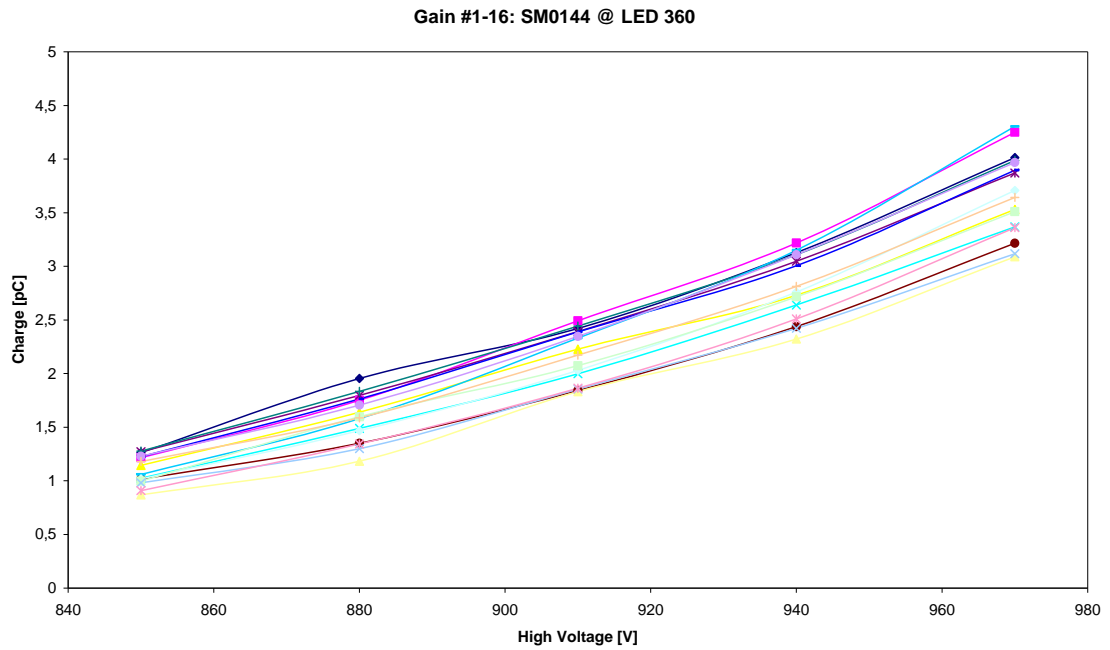


Figure 2.18 Gain of 16 channels of SM0144 at 360 nm LED.

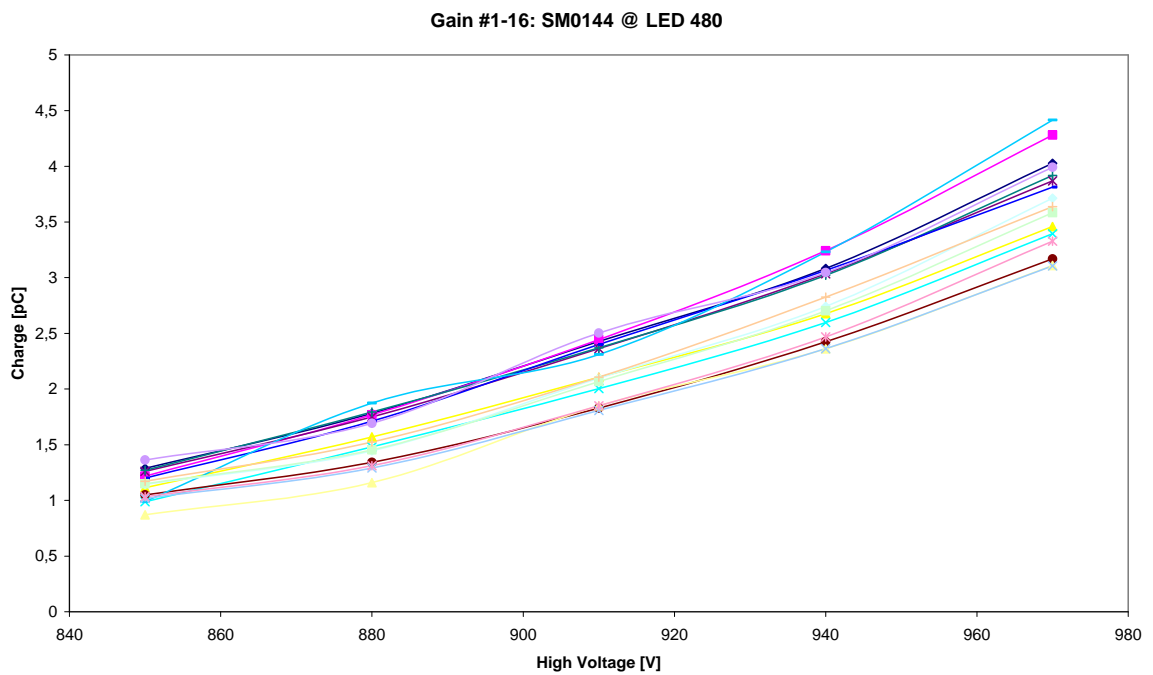


Figure 2.19 Gain of 16 channels of SM0144 at 480 nm LED.

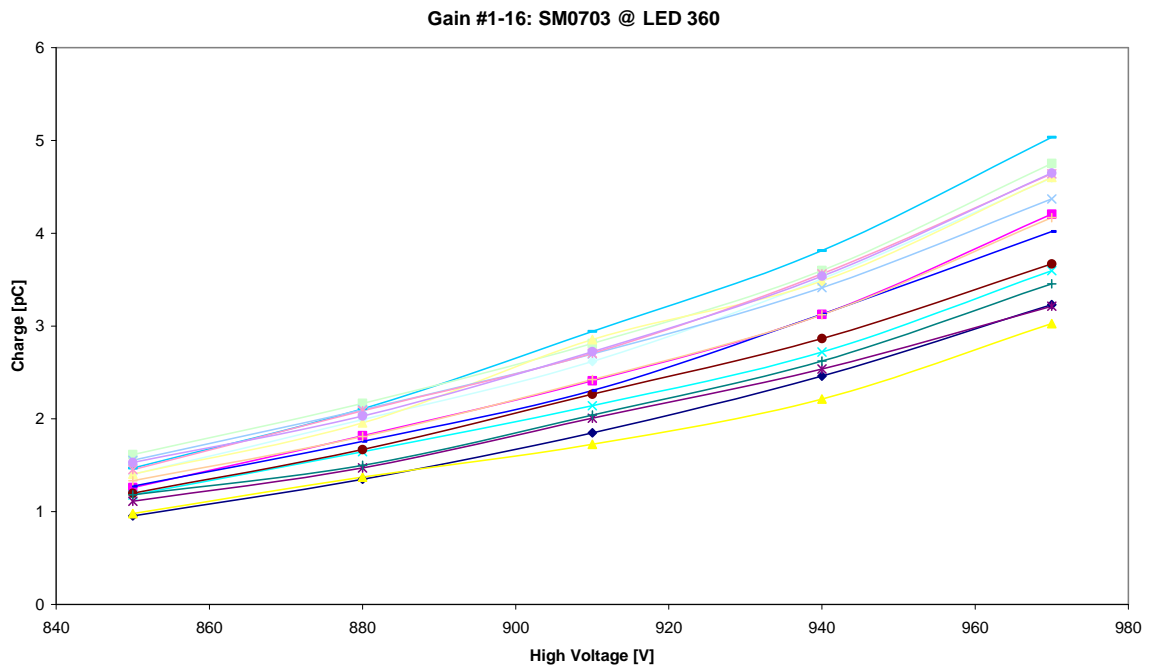


Figure 2.20 Gain of 16 channels of SM0703 at 360 nm LED.

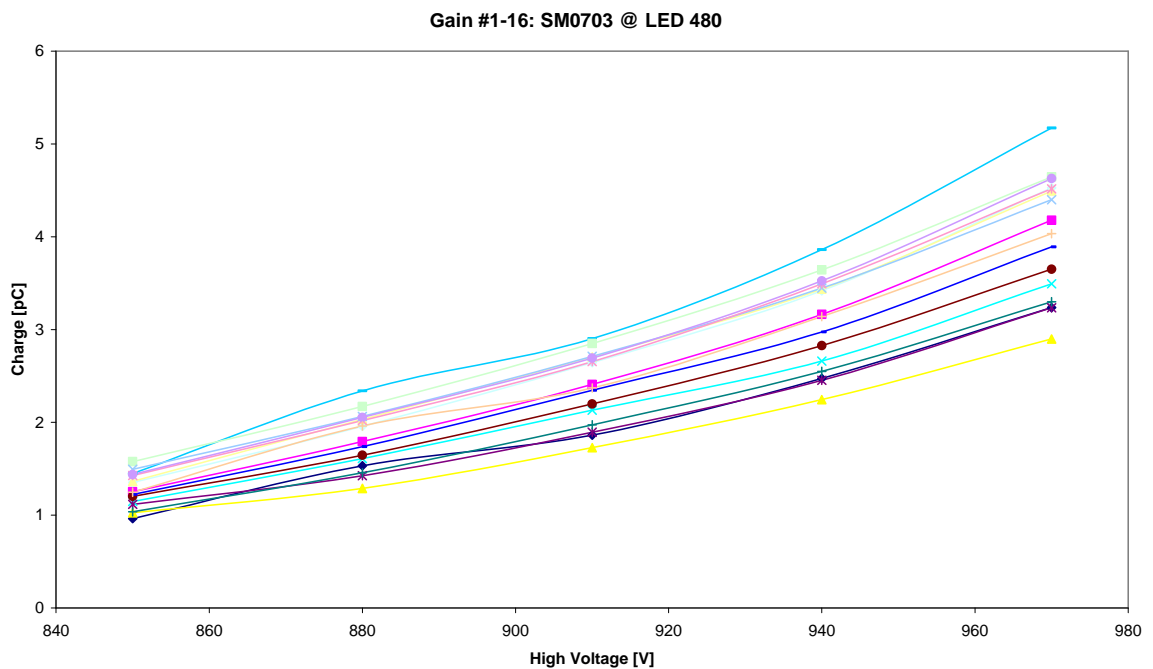


Figure 2.21 Gain of 16 channels of SM0703 at 480 nm LED.

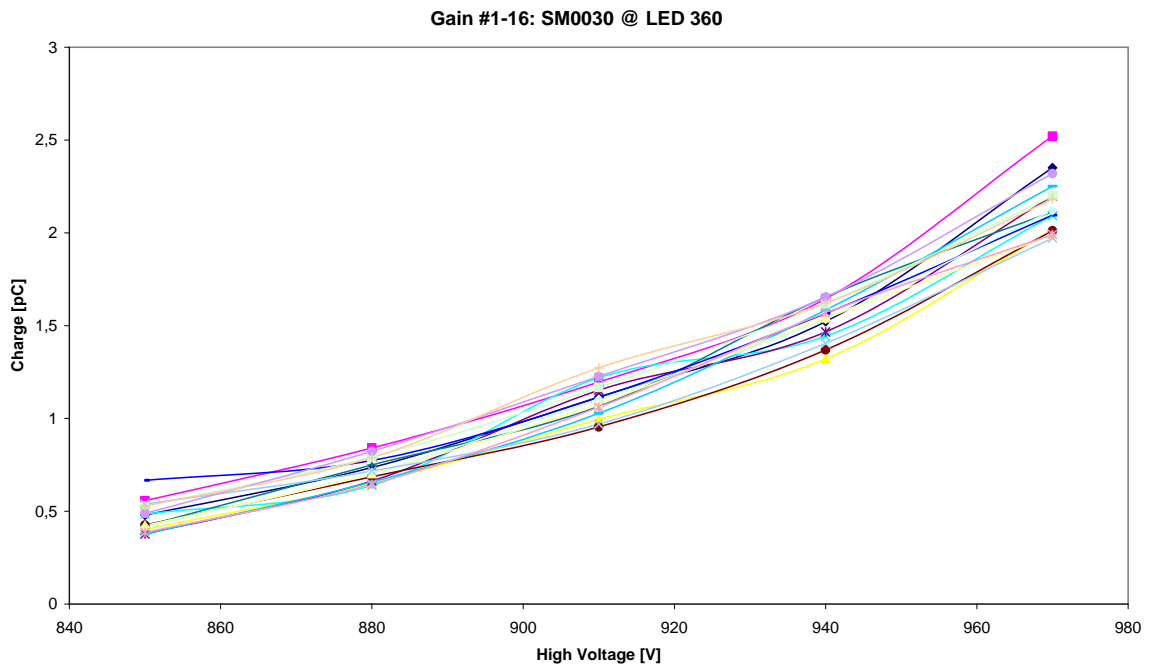


Figure 2.22 Gain of 16 channels of SM0030 at 360 nm LED.

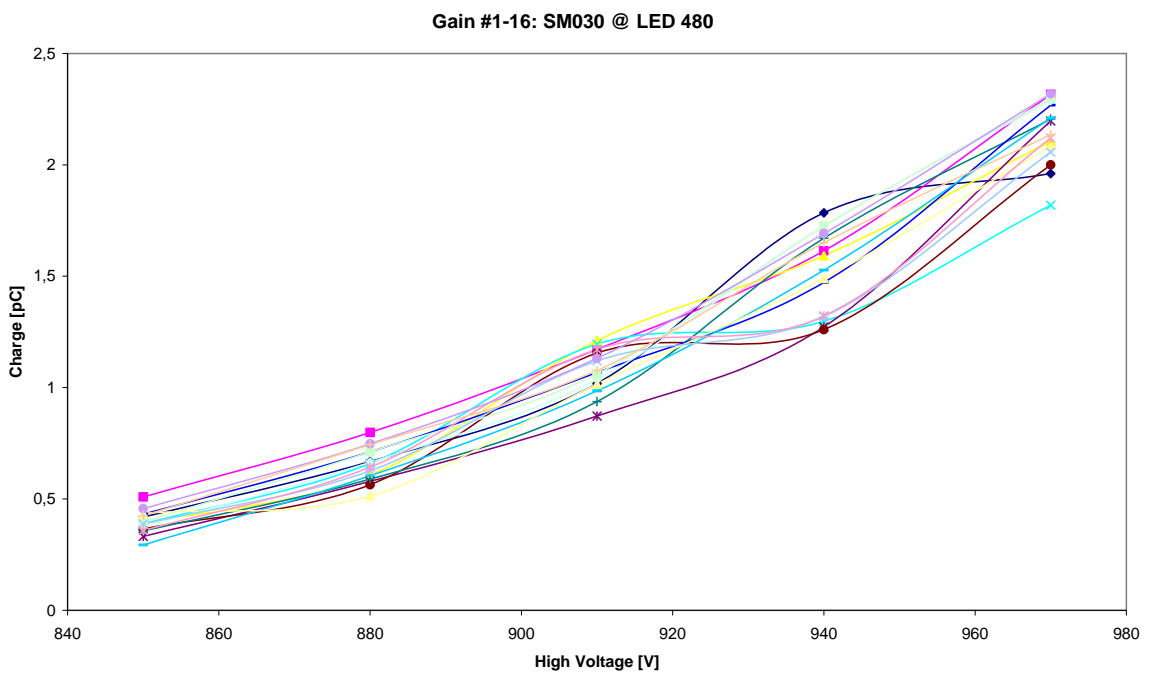


Figure 2.23 Gain of 16 channels of SM0030 at 480 nm LED.

Now Gain ratio is made for one PMT to see differences between 360 nm and 480 nm LEDs. The ratio should be about one to proof that PMT work as an ideal amplifier (Fig. 2.24 – SM0144).

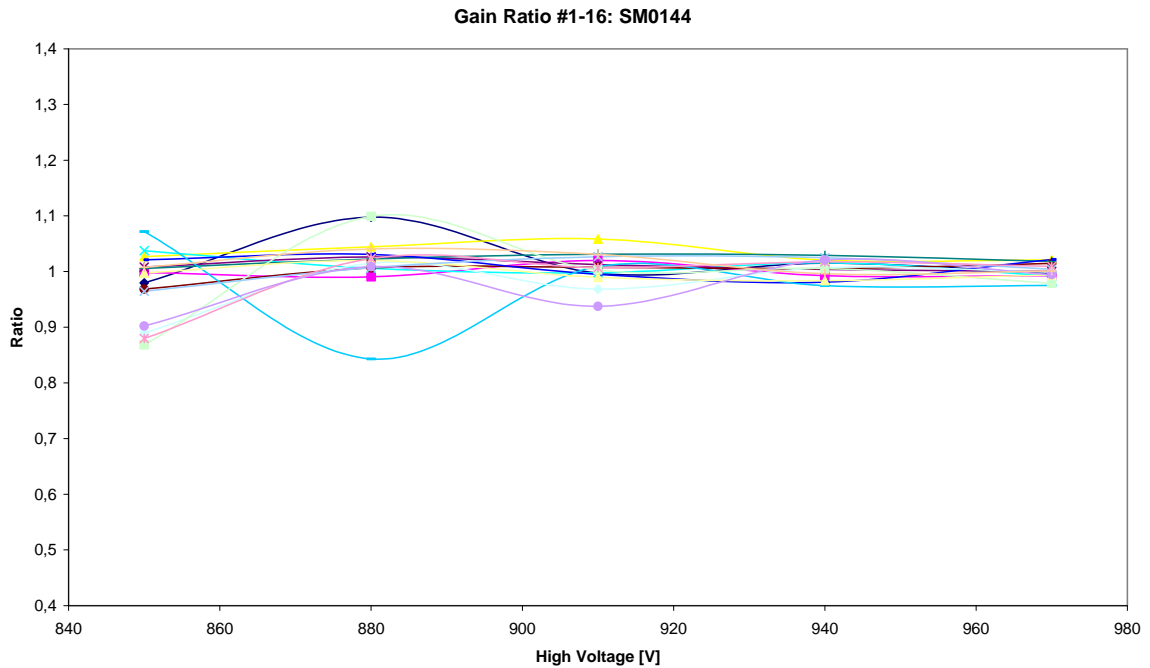


Figure 2.24 Gain Ratio of 16 channels of SM0144.

Gain was not measured separately but we could get values from the raw data. From shown histograms it is possible to get mean value of the main peak and this value serves for determination of gain. Spectra are fitted a Gaussian-curve (Eq. 2.4).

$$f(x) = P_0 \exp\left(-0.5 \cdot \left(\frac{x - P_1}{P_2}\right)^2\right) \quad \text{Eq. 2-4}$$

P_0 is height of the peak.

P_1 is mean of the peak.

P_2 is sigma of the peak.

I should only add information that all graphs for gain are shown with pedestal correction. That means the pedestal position is subtracted from the position of mean value of main peak.

Quantum efficiency

Relative quantum efficiency could be also evaluated from raw data. Relative quantum efficiency is yield ratio between 360 nm and 480 nm LEDs. Counted area is from crosstalks (inclusive) up to mean value of the main peak plus one sigma. This area is marked with green color on figure 2.12.

Results are shown for three selected PMTs. These are the same as before (Fig. 2.25 – SM0144, Fig. 2.26 – SM0703, Fig. 2.27 – SM0030).

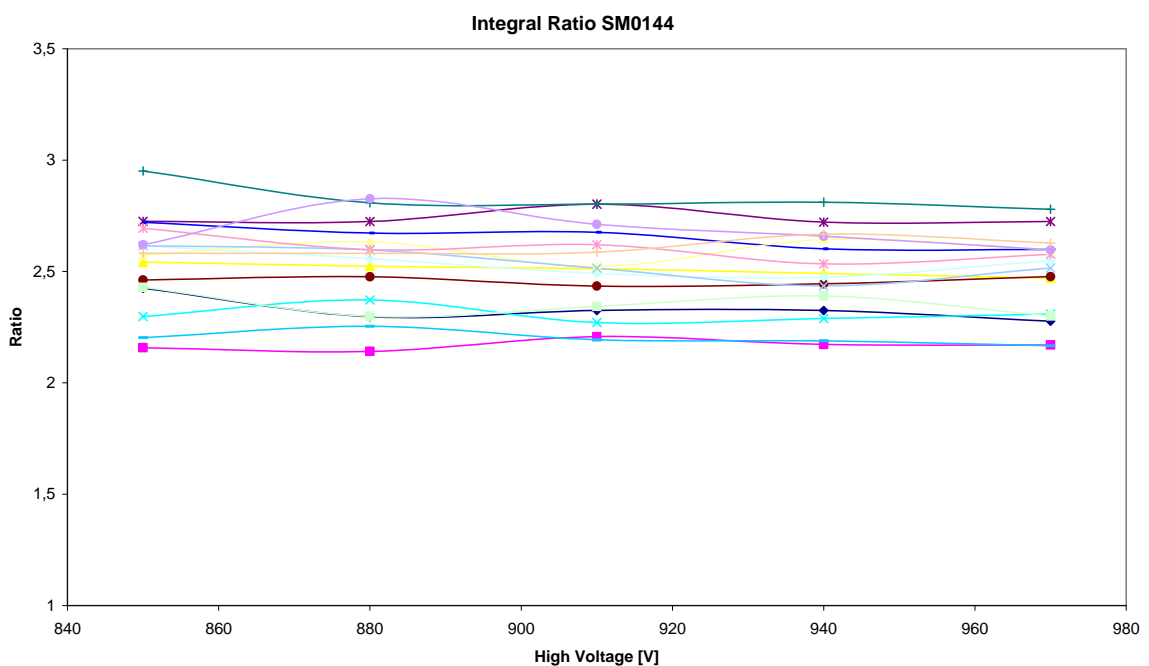


Figure 2.25 Integral Ratio of quantum efficiency at 360 nm and 480 nm of 16 channels of SM0144.

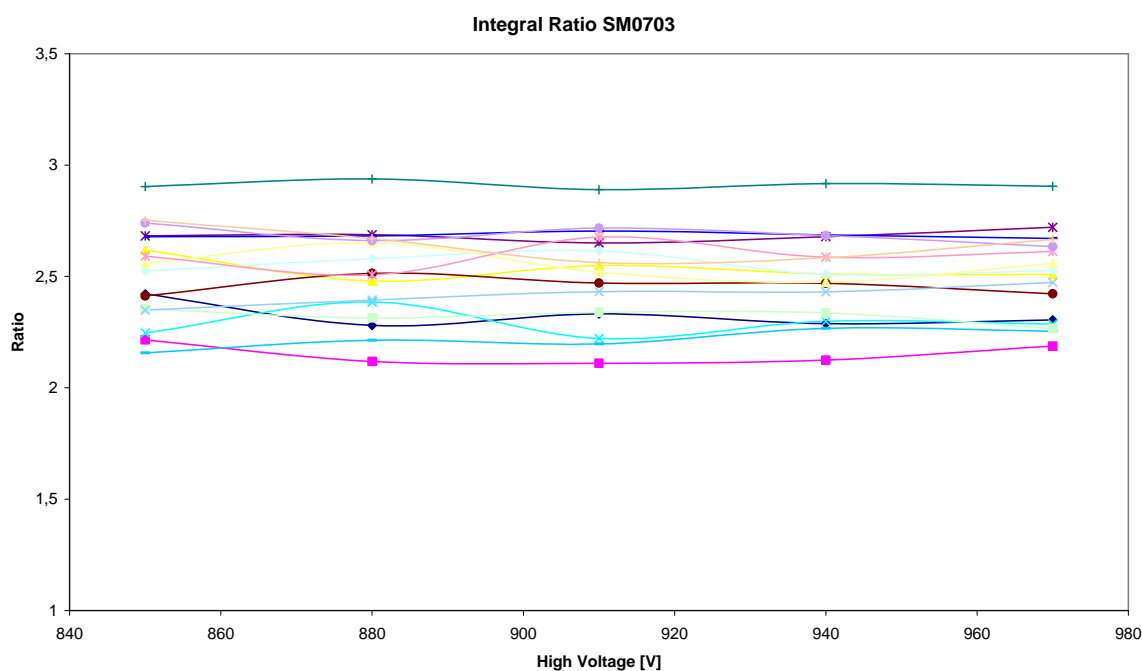


Figure 2.26 Integral Ratio of quantum efficiency at 360 nm and 480 nm of 16 channels of SM0703.

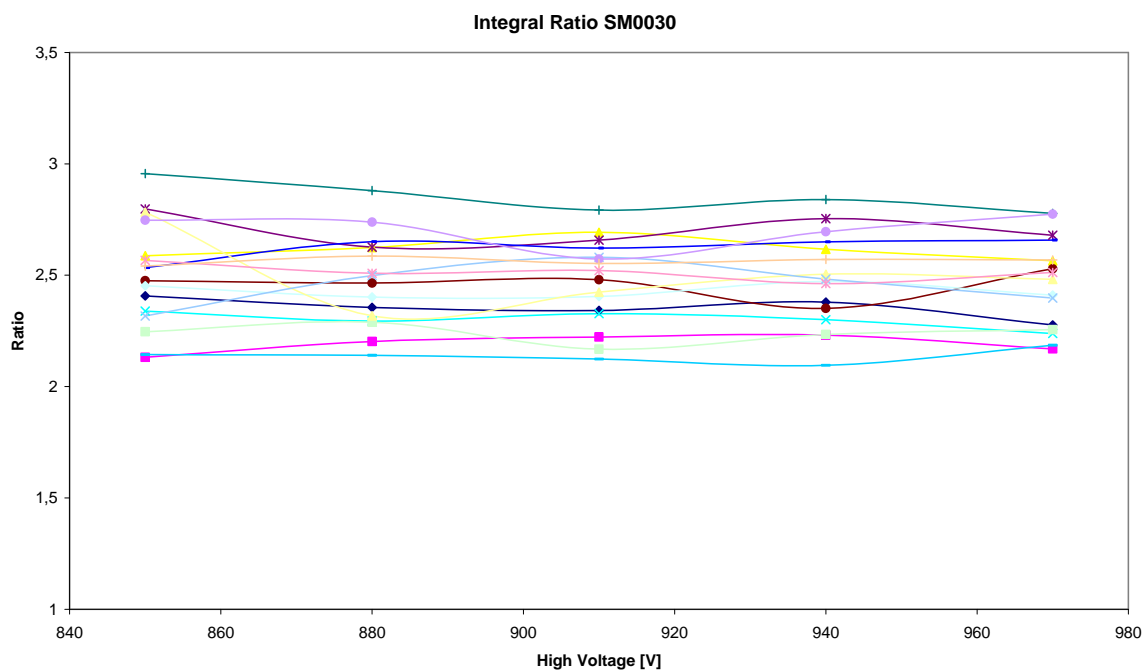


Figure 2.27 Integral Ratio of quantum efficiency at 360 nm and 480 nm of 16 channels of SM0030.

Uniformity

Response of one PMT was a little bit different among channels. We should watch this difference to be sure that channels are similar to each other till certain ratio. It is important for following result processing in the RICH detector.

On figure 2.28 is shown normalized histogram of uniformity in channel one.

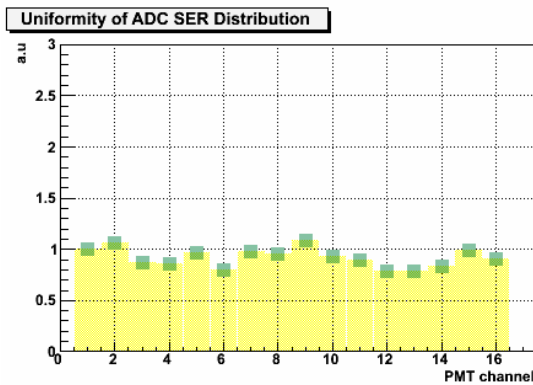


Figure 2.28 Histogram of all channels uniformity normalized to channel one for SM0144.

During our tests some other plots were made (Fig. 2.29). Mean of the charge distribution (Y-axis is multiplied by ten), next was recorded parameter sigma of Gaussian distribution for main peak, also uniformity and normalized integral are recorded. Last two plots represented ratio between first channel and remaining channels.

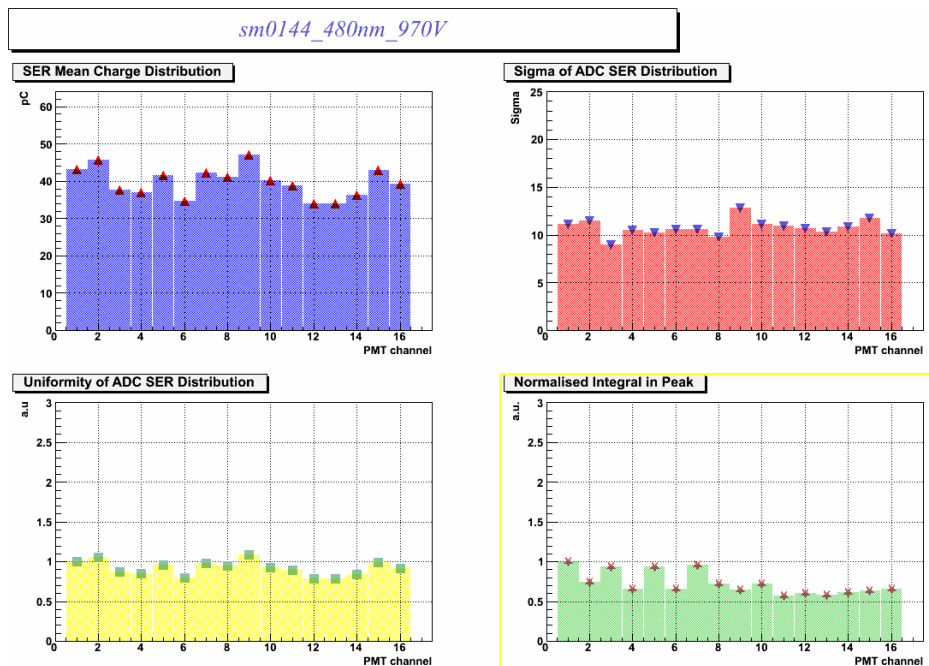


Figure 2.29 Additional outcome plots for SM0144.

Crosstalks

Crosstalk is a measure to indicate how accurately the light incident on a certain position of the photocathode is detected with the position information still retained. In PMT operation, crosstalk is mainly caused by the broadening of electron flow when light is converted into electrons and those electrons are multiplied in the dynode section. The incident light spread within the faceplate is another probable cause of crosstalk [7].

Crosstalk's survey is made from already collected data. Root program serves to find out these outcomes. Used algorithm firstly organizes data to a histogram, and then calibrates them to equivalent pedestal position. For channel took as reference one program takes data according to mean position of the main peak ± 3 sigma and for the rest program counts only data from pedestal until the mean position -3 sigma. But counted data are only these, where value is highest from all channels for specific event. These results are only approximate. Crosstalks on neighboring channels are below 2 % of the main channel (Fig. 2.30).

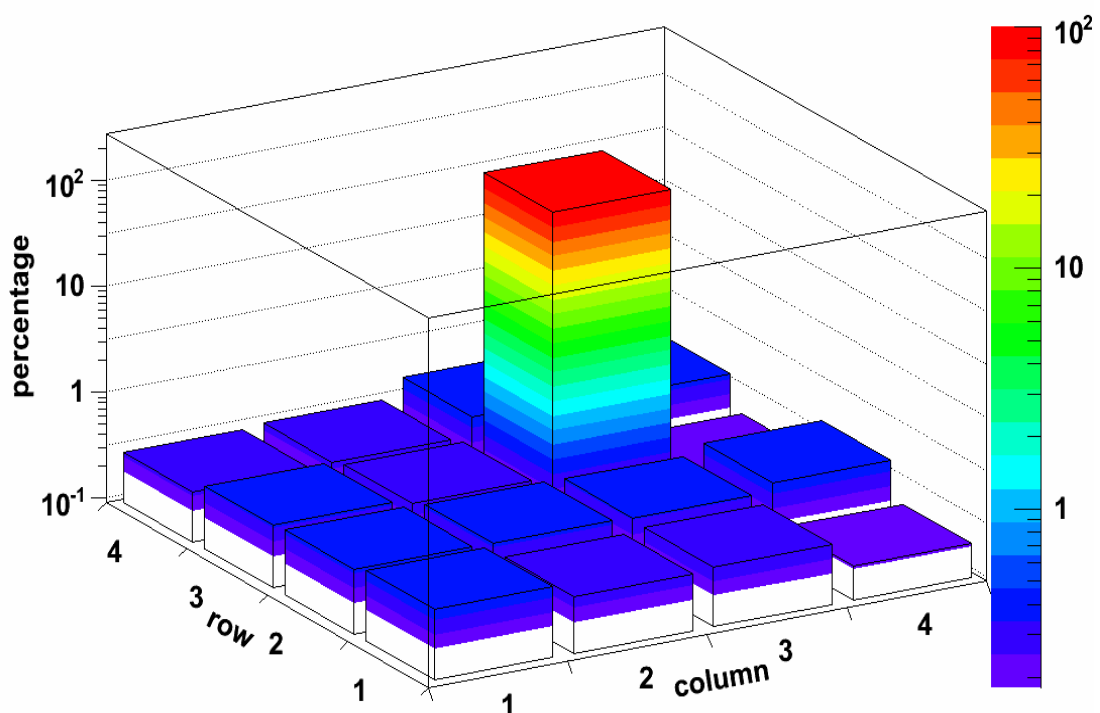


Figure 2.30 3D Crosstalks for SM0144_480nm_970V - channel 10.

Some additional graphs are also made in the program (Fig. 2.31). Here are shown only these important, but in `<SM0144_480nm_970V_cross.ps>` is the rest. Obtained values are stored in file on hard disk.

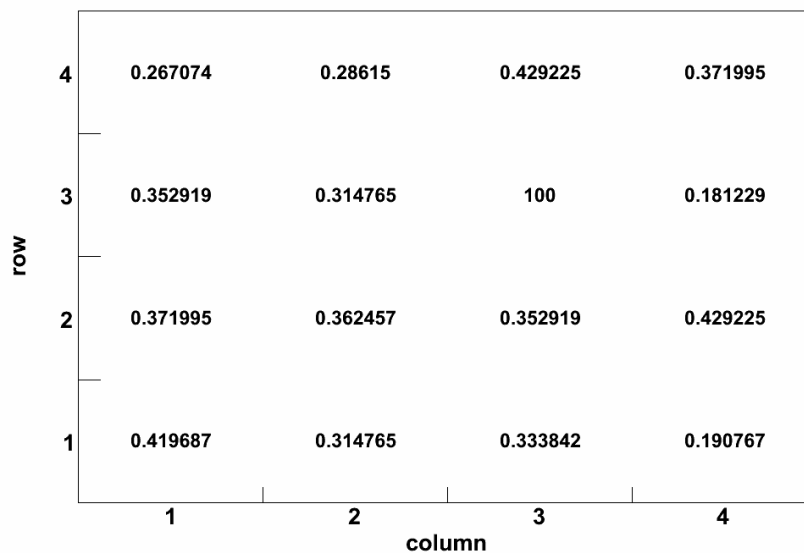


Figure 2.31 Crosstalks in numbers for *SM0144_480nm_970V - channel 10*.

3 Discussion

The set of 594 multi-anode photomultipliers was tested. Tests proceedings are enclosed in appendix B. Also according to outcomes it was said which PMT is going to be used in the RICH1 detector and which one doesn't meet given criteria. This will be discussed in following rows.

The highest criterion is given for dark current measurement. In order to minimize the probability of random trigger in the detector, PMTs with high dark noise rate were rejected. Dark current should not exceed 2 nA per channel.

The gain of one channel, respectively the mean value of main peak, should not be under 1 pC per channel. According to achieved results all PMTs are above this limit. But this condition is accomplished only for some voltages. Maximal impress voltage for one PMT is 1000 V. Each photomultiplier which will be used in the detector will have its own power supply. So it is possible to change voltage for each one separately and according to best yields. But electronics around PMT is proposed to be used in range from 850 V to 900 V. And not all PMTs have sufficient yield at these low feedings. Therefore PMTs should be divided into at least three sections by their yields (gain).

I have made a histogram (Fig. 2.32), where average mean charge of PMT is shown for all tested photomultipliers. Values on X-axis are not calibrated (to calibrate these data, mean charge should be decreased about pedestal and then divided by ten to get real mean value). I haven't made it, because mean charge values for each channel of PMTs are stored without this calibration too. So it is easier to sort PMTs according to values in this histogram, made for 880 V. I propose to sort PMTs to three groups. The first section of PMTs has mean charge till 10 pC and it should be connected to 900 V (at least). The second part should be connected to 880 V. All PMTs with mean charge from 10 to 20 pC should be in this section. The rest (20 pC and more) comprises third section. Because of high mean charge and gain dependency shown in previous chapter, PMTs from the third section could be connected to 850 V. Then PMTs connected in the RICH detector could work with similar outputs (spectral response). The first section includes 11 % of all PMTs, the second section includes 68 % and in the last section are 21 % of tested PMTs.

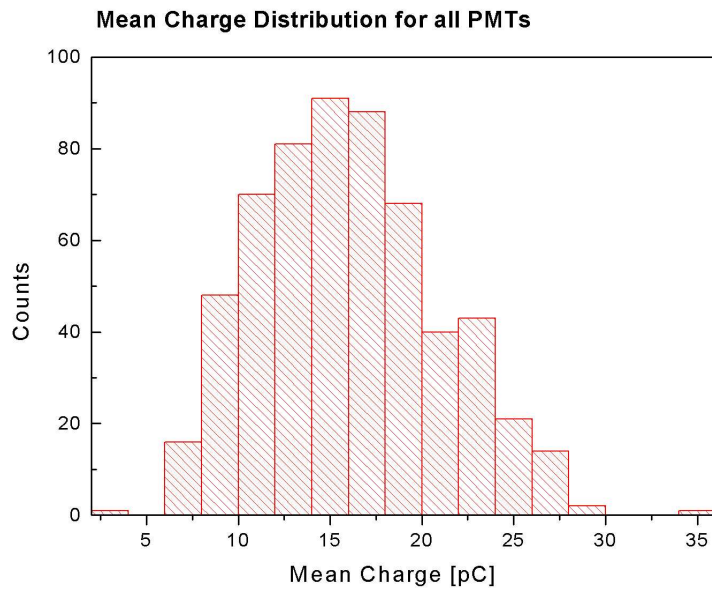


Figure 2.32 Mean Charge distribution for all PMTs.

Then PMTs should be also placed in certain positions by this classification. PMTs with low signal should be placed somewhere of the less important places in the detector.

Channels response for one photon (our measuring conditions) is different for each of them. This difference (ratio between channels) should not be higher than 3. But one problem for appraisal of the uniformity has occurred. We found that if we change PMT position in the holder (turning about specific angle), shown spectrum will change (Fig 2.33).

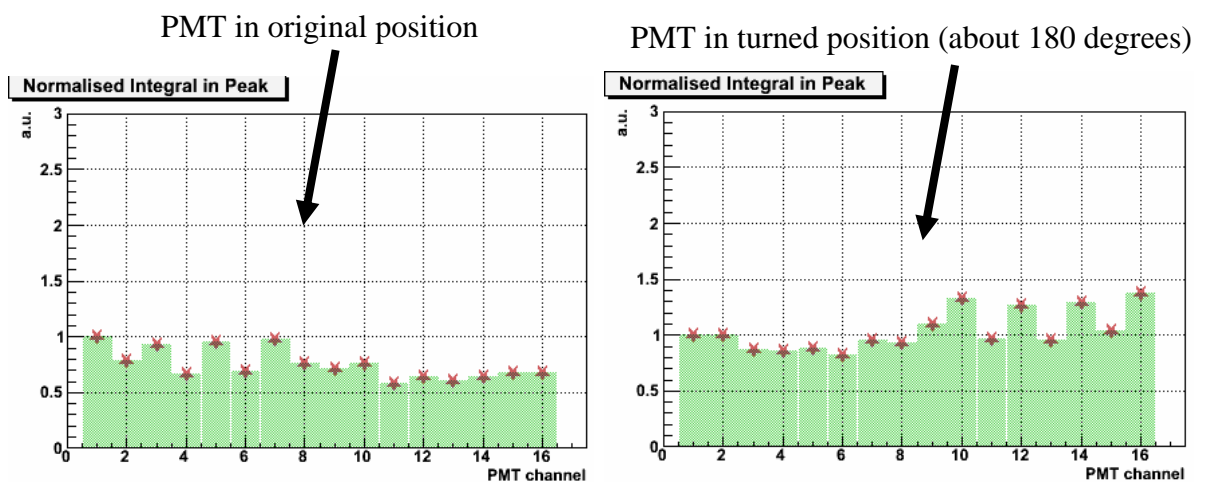


Figure 2.33 Normalized integral in peak of SM0784 for normal position in PMT holder and for turned PMT about 180 degrees.

This difference is caused because light wasn't spread homogenously. To solve this problem and to judge each PMT from this point of view it should be done some additional measurements. These measurements should be done for few PMTs but each of them should be measured in different position. After these measurements we would be able to calculate some coefficient for non homogenous light and then adjust given values for each PMT only. It could be done with some script for ROOT analysis framework. For now we could at least average all data corresponded to specific channel. Then we could judge variances between each channel and the average value. But this is confrontal between PMTs and we would like to get confrontal between channels of one PMT and besides this variations will only show channel difference from average gain of selected channel.

The measurement of crosstalk is only estimative. If we would like to get more precise information we should illuminate only one pad of the PMT. But in our measurement whole photocathode can be illuminated. Illuminating exact position is possible by using a scintillation fiber. Fiber should be bringing into tight contact with the photomultiplier tube faceplate to make accurate measurement. Typical crosstalk measurement method is shown on figure 2.34.

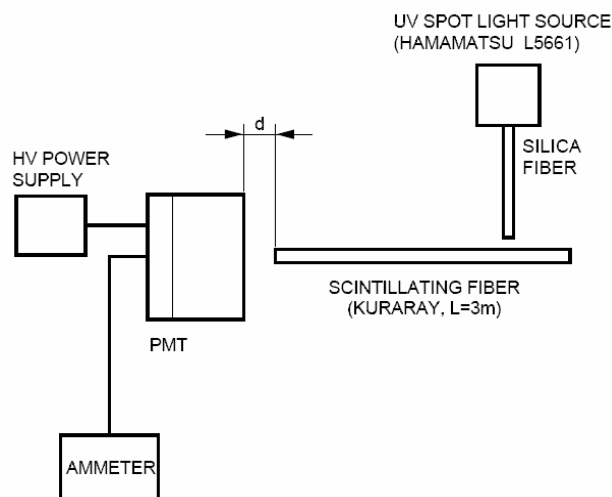


Figure 2.33 *Crosstalk measurement method [7].*
(“*d*” should be zero to make exact measurement.)

Conclusions

Aims of this Diploma Thesis were accomplished. Measurement method was adapted and important qualities of multi-anode photomultipliers were measured.

During preliminary measurements I participated on measuring method adaptation. Firstly it was necessary to reduce LED's light yield to get single photon regime and find optimum range of impress voltage. Time to recover original level of Dark Current was determined too. Secondary outcomes of measurements were discussed and agreed.

We measured 594 photomultipliers after measurement method adjustments. I measured 150 PMTs myself. Some PMTs with high noise level were rejected. I sorted all tested PMTs to three groups according to their average mean charge. PMT's tested parameters met our expectation. Crosstalks with 1 % level are acceptable. Gain and Dark Current were also in conformity with manufacturer's assertion. Finally I participated on data analysis.

All selected PMTs are now placed to RICH detector, connected to power suppliers and their functionality was checked. The rebuilt RICH detector will be able to detect particles in June, 2006.

Literature

- [1] M. Alekseev et al.: Studies for a fast RICH. Nuclear Instruments and Methods in Physics Research Section A: Accelerators, Spectrometers, Detectors and Associated Equipment, 55 (2005) 53-57
- [2] Kramer, D.: Optical concentrators for Cherenkov light detector. [Diploma thesis] Liberec 2005, Technical university of Liberec.
- [3] Albrecht E. et al.: A prototype RICH detector using multi-anode photomultiplier tubes and hybrid photo-diodes. Nuclear Instruments and Methods in Physics Research Section A: Accelerators, Spectrometers, Detectors and Associated Equipment, 456 (2001) 233-247
- [4] Knoll, G.F.: Radiation Detection and Measurement, John Wiley and Sons, 2000, ISBN 0-471-07338-5
- [5] Aufderheide, K. - Forensic science [online]. c2004, [cit. 2006-05-05]. < http://www.oglethorpe.edu/faculty/~k_aufderheide >.
- [6] Molecular Expressions Microscopy Primer: Photomicrography [online]. c2000, last revision 21st of July 2004 [cit. 2006-05-05]. < <http://microscopy.fsu.edu/> >.
- [7] HAMAMATSU Photonics k.k.: Photomultiplier Tubes – Basics and Applications. Japan 1999, Hamamatsu Photonics k.k.
- [8] Photomultiplier Catalogue Hamamatsu.
- [9] Stanovik A. et al, Tests of a multianode PMT for the HERA-B RICH, Nuclear Instruments and Methods in Physics Research A 394 (1997) 27-34
- [10] Póltorak, K.: THE TESTS OF THE ATLAS TILE CALORIMETER PHOTOMULTIPLIERS. [Diploma thesis.] Krakov 2004, AGH University of Science and Technology Faculty of Physics and Nuclear Techniques.
- [11] HAMAMATSU Photonics k.k.: Multianode photomultiplier tube assembly H6568, H6568-10. [Data sheet] Japan, Hamamatsu Photonics k.k.